

Ruthenium-Stabilized Low-Coordinate Phosphorus Atoms. *p*-Cymene Ligand as Reactivity Switch

Richard Menye-Biyogo,[‡] Fabien Delpech,^{*‡,§} Annie Castel,[‡] Véronique Pimenta,[†]
Heinz Gornitzka,[‡] and Pierre Rivière[‡]

Laboratoire Hétérochimie Fondamentale et Appliquée, UMR 5069, Université Paul Sabatier, 118 Route de Narbonne, 31062 Toulouse Cedex 09, France, and Laboratoire des Interactions Moléculaires et Réactivité Chimique et Photochimique, UMR 5623, Université Paul Sabatier, 118 Route de Narbonne, 31062 Toulouse Cedex 09, France

Received May 16, 2007

A detailed comparative study of the structural and spectroscopic features and of the reactivity of ruthenium phosphinidene complexes (η^6 -Ar)(PCy₃)Ru(PMes*) (**2a**, Ar = *p*-cymene; **2b**, Ar = benzene) has been undertaken. The structures of complexes **2a** and **2b** have been determined by single-crystal X-ray diffraction and display similar features. Both compounds possess identical chemical behavior toward Brønsted acids such as HBF₄: protonation of the phosphinidene ligand yields the new cationic complexes [(η^6 -Ar)(PCy₃)Ru(PHMes*)]BF₄ (**3aBF₄**, Ar = *p*-cymene; **3bBF₄**, Ar = benzene), which exhibit an unprecedented phosphonium-bearing hydrogen substituent. **3aBF₄** has been characterized using X-ray diffraction techniques. The lone pair of the phosphorus atom of the phosphinidene ligand remains also accessible to the Lewis acid BH₃: the reactions of **2a** and **2b** with borane give the adducts (η^6 -Ar)-(PCy₃)Ru[P(BH₃)Mes*] (**4a**, Ar = *p*-cymene; **4b**, Ar = benzene). In the presence of the larger borane BPh₃, no reaction occurs until water is introduced in the reaction vessel. This results in the generation of [(η^6 -Ar)(PCy₃)Ru(PHMes*)]BPh₃OH (**3aBPh₃OH**, Ar = *p*-cymene; **3bBPh₃OH**, Ar = benzene) presumably through protonation of **2a** and **2b** by the previously unknown adduct H₂O·BPh₃. Phosphinidene complexes react also with electrophilic alkylating reagents such as organic iodides provided the alkyl substituent is small. Treatment of **2a** and **2b** with 1 equiv of methyl iodide leads to the alkylation at the phosphinidene center and yields the phosphonium complexes [(η^6 -Ar)(PCy₃)Ru(PMeMes*)]I (**5a**, Ar = *p*-cymene; **5b**, Ar = benzene). Examination of the reactivity toward electron-rich reagents such as the alkynes RCCH (R = Me₃Si, Ph) yields unexpected results: **2a** instantaneously reacts to generate phosphindane complexes **6** and **7**, whereas no reaction occurs when using **2b**. A detailed kinetic study provides evidence for a dissociative mechanism involving the release of the phosphine ligand in **2a** and explains its specificity. The *p*-cymene ligand in **2a** acts as a reactivity switch due to the higher steric hindrance of this arene.

Introduction

Transition metal-catalyzed carbon–heteroatom bond formation is a fundamental process in chemical synthesis.¹ Among the existing methodologies, catalyzed atom transfer plays a pivotal role and has stimulated the tremendous development of the chemistry of carbene, imido, and oxo complexes.² In this context, phosphinidene complexes have attracted considerable attention since their existence was evidenced.³ In the last two decades, these efforts have resulted in significant progress exemplified by the first structural characterization of terminal phosphinidene complexes.⁴ These advances have stimulated the

development of strategies for the generation of phosphinidene in the coordination sphere of transition metals.⁵ Thus, several pathways are currently available and have allowed preparation and full characterization of phosphinidene complexes incorporating different transition metals (Ti,⁶ Zr,⁷ V,⁸ Ta,⁹ Mo,¹⁰ W,¹¹ Re,¹² Fe,¹³ Ru,^{14,15} Os,¹³ Co,¹⁶ Rh,¹⁶ Ir,¹⁷ Ni¹⁸). From a synthetic

* Author to whom the correspondence should be addressed. E-mail: fdelp@insa-toulouse.fr.

[‡] Laboratoire Hétérochimie Fondamentale et Appliquée.

[†] Laboratoire des Interactions Moléculaires et Réactivité Chimique et Photochimique.

[§] Present address: Laboratoire de Physique et Chimie des Nano-Objets, Département de Génie Physique, Institut National des Sciences Appliquées, 135 Avenue de Rangueil, 31077 Toulouse Cedex 04, France.

(1) (a) Han, L. B.; Tanaka, M. *Chem. Commun.* **1999**, 395–402. (b) Bedford, R. B.; Cazin, C. S. J.; Holder D. *Coord. Chem. Rev.* **2004**, *248*, 2283–2321.

(2) Nugent, W. A.; Mayer, J. M. *Metal-Ligand Multiple Bonds*; Wiley: New York, 1989.

(3) Mathey, F. *Angew. Chem., Int. Ed. Engl.* **1987**, *26*, 275–286.

(4) Cowley, A. H. *Acc. Chem. Res.* **1997**, *30*, 445–451.

(5) (a) Dillon, K. B.; Mathey, F.; Nixon, J. F. *Phosphorus: The Carbon Copy*; Wiley: Chichester, 1998; Chapter 3. (b) Lammertsma, K. Phosphinidenes. In *Topics in Current Chemistry: New Aspects in Phosphorus Chemistry III*; Springer: Berlin, 2003; Vol. 229, pp 95–119. (c) Mathey, F. *Angew. Chem., Int. Ed.* **2003**, *42*, 1578–1604.

(6) Basuli, F.; Tomaszewski, J. C.; Huffman, J. C.; Mindiola, D. J. *J. Am. Chem. Soc.* **2003**, *125*, 10171–10172.

(7) Hou, Z.; Breen, T. L.; Stephan, D. W. *Organometallics* **1993**, *12*, 3158–3167.

(8) Basuli, F.; Bailey, B. C.; Huffman, J. C.; Baik, M.-H.; Mindiola, D. J. *J. Am. Chem. Soc.* **2004**, *126*, 1924–1925.

(9) Cummins, C. C.; Schrock, R. R.; Davis, W. M. *Angew. Chem.* **1993**, *105*, 758–761.

(10) Hitchcock, P. B.; Lappert, M. F.; Leung, W. P. *J. Chem. Soc., Chem. Commun.* **1987**, 1282–1283.

(11) Cowley, A. H.; Pellerin, B.; Atwood, J. L.; Bott, S. G. *J. Am. Chem. Soc.* **1990**, *112*, 6734–6735.

(12) Graham, T. W.; Cariou, R. P. Y.; Sánchez-Nieves, J.; Allen, A. E.; Udachin, K. A.; Regragui, R.; Carty, A. J. *Organometallics* **2005**, *24*, 2023–2026.

standpoint, only terminal phosphinidene complexes are of major interest since bridging phosphinidenes display little reactivity in a μ_2 -, μ_3 -, or μ_4 -bridging modes except in rare cases.¹⁹ Terminal phosphinidene complexes exist in two varieties, which display electrophilic Fisher-type or nucleophilic Schrock-type properties and, thus, mimic their carbene analogues. A recent computational study has shown that, in addition to the ancillary ligands on the metal, both the charge on the complex and the nature of the phosphinidene substituents can significantly influence electro- or nucleophilicity.²⁰

Surprisingly, despite the considerable attention fueled by the analogy with carbene, direct involvement of phosphinidene in catalytic processes has been demonstrated in only two cases.²¹ Similarly, studies concerning the synthetic potential of phosphinidene complexes are still very rare except in the case of the transient *in situ* generated complex (CO)₅W(PPh). The phosphorus atom exhibits electrophilic properties, and the numerous examples of addition to olefinic and acetylenic systems have been reviewed recently.²² In contrast, little of the chemical behavior of nucleophilic phosphinidene complexes has been explored, the most documented one being Cp₂(PMe₃)Zr-(PMe₃)^{*} (Mes^{*} = 2,4,6-tri-*tert*-butylphenyl). The characteristic reactions are 1,2-additions with protic reagents, [2+2] cycloadditions with alkynes leading to phosphametallacycles,^{4,23,24} and the phospho-Wittig reaction with carbonyl compounds.^{4,9,24} Comparatively, group 9 metal phosphinidene complexes of general formula Cp^{*}(PPh₃)M(PMe₃)^{*} (M = Co, Rh, Ir) exhibit poor reactivity, reacting only with organic iodides. DFT calculations showed that the lower nucleophilicity of the phosphorus atom accounts largely for such a discrepancy with the reactivity of the related zirconium complexes.¹⁶ Additionally, in the latter case, the facile dissociation of the PMe₃ ligand also appears crucial for explaining its unique reactivity.²⁵

We have recently reported the synthesis and the first structural evidence for monomeric metaphosphonate by taking advantage of the high reactivity of the phosphinidene complex (η^6 -*p*-cymene)(PCy₃)Ru(PMe₃)^{*} (*p*-cymene = 4-methylisopropyl-

benzene).²⁶ As a part of our ongoing studies of the reactivity of phosphinidene complexes, we examined the behavior (η^6 -Ar)(PCy₃)Ru(PMe₃)^{*} (Ar = *p*-cymene, benzene) toward electrophilic reagents and alkynes. Surprisingly, in the latter case, the benzene ligand derived complex did not react, while total consumption of (η^6 -*p*-cymene)(PCy₃)Ru(PMe₃)^{*} was immediately observed. To the best of our knowledge, there is no example in the literature reporting that benzene and the *p*-cymene ligand could induce such different behaviors of the corresponding organometallic complexes. This prompted us to investigate in depth their structural and chemical features. In this paper, we describe (i) the full characterization of these phosphinidene complexes and (ii) their respective reactivity toward electrophilic and electron-rich reactants in order to identify the exact origin of this contradictory behavior. This comparative analysis addresses this issue, and we will show how subtle structural changes result in dramatic enhancement of the reactivity of such species.

Results and Discussion

Synthesis, Spectroscopic, and Structural Characterization. The ruthenium-complexed terminal phosphinidenes were synthesized using the base-induced dehydrohalogenation–ligation sequence described by Lammerstma et al.¹⁷ The reaction of (η^6 -Ar)(PH₂Mes^{*})RuCl₂ (**1a**, Ar = *p*-cymene; **1b**, Ar = benzene) with 2 equiv of 1,8-diazabicyclo[5.4.0]undec-7-ene (DBU) in the presence of PCy₃ afforded (η^6 -Ar)(PCy₃)Ru-(PMe₃)^{*} (**2a**, Ar = *p*-cymene; **2b**, Ar = benzene) as water-stable green crystals in high yields. Their ³¹P, ¹³C, and ¹H NMR spectra display nearly identical signals (Scheme 1). The high-field ³¹P NMR resonances (δ 813 for **2a** and δ 819 for **2b**) for the phosphorus atom of the phosphinidene ligand are in the typical region for terminal phosphinidene complexes.⁵ The slight shielding of this chemical shift in **2a** is also observed for the PCy₃ resonance (δ 35 for **2a** and δ 38 for **2b**). This minor difference can be attributed to the slight donating effect of *p*-cymene, compared to that of the benzene ligand. A similar trend is observed for (η^6 -Ar)(PPh₃)Ru(PMe₃)^{*}.^{15,27} The η^6 -Ar ligand and the Mes^{*} moiety are in free rotation in complexes **2** since no decoalescence is observed for the aryl or the methyl protons in the ¹H NMR spectra, even at low temperature.

X-ray diffraction analyses of both complexes were then conducted. The solid-state structures of **2a** and **2b** are shown in Figure 1 and reveal very similar features. The environment of the ruthenium atom is congested, and the X-ray structure shows a long Ru–PCy₃ bond (2.386(4) Å for **2a** and 2.389(7) Å for **2b**) and a short Ru–PMe₃^{*} one (2.205(3) Å for **2a** and 2.237(7) Å for **2b**). The short Ru–PMe₃^{*} distances together with the acute angles Cy₃P–Ru–PMe₃^{*} (85.98(14)° for **2a** and 86.7(3)° for **2b**) and Ru–P–C_{ipso}(Mes^{*}) (110.5(4)° for **2a** and 107.6(8)° for **2b**) are characteristic for terminal bent phosphinidene complexes. Concerning these angles, the difference between **2a** and **2b** can be rationalized in terms of steric repulsion between the arene ligand and Mes^{*} substituent. However, these variations are minor and both structures very much resemble that of (η^6 -*p*-cymene)(PPh₃)Os(PMe₃)^{*} and (η^6 -benzene)(PPh₃)Ru(PMe₃)^{*}.¹⁵

Since the physical properties provide no clear evidence to rationalize the different behavior between **2a** and **2b**, a detailed reactivity study was undertaken in order to gain some insight.

(26) Menye Biyogo, R.; Delpech, F.; Castel, A.; Riviere, P.; Gornitzka, H. *Angew. Chem., Int. Ed.* **2003**, *42*, 5610–5612.

(27) Menye-Biyogo, R. Terminal Phosphinidene Ruthenium Complexes: Synthesis and Reactivity. Ph.D. dissertation, University Paul Sabatier, Toulouse, France, November 2005.

(13) Sterenberg, B. T.; Udachin, K. A.; Carty, A. J. *Organometallics* **2003**, *22*, 3927–3932.

(14) Sterenberg, B. T.; Udachin, K. A.; Carty, A. J. *Organometallics* **2001**, *20*, 2657–2659.

(15) Termaten, A. T.; Nijbacker, T.; Schakel, M.; Lutz, M.; Spek, A. L.; Lammertsma, K. *Chem. Eur. J.* **2003**, *9*, 2200–2208.

(16) Termaten, A. T.; Aktas, H.; Schakel, M.; Ehlers, A. W.; Lutz, M.; Spek, A. L.; Lammertsma, K. *Organometallics* **2003**, *22*, 1827–1835.

(17) Termaten, A. T.; Nijbaker, T.; Schakel, M.; Lutz, M.; Spek, A. L.; Lammertsma, K. *Organometallics* **2002**, *21*, 3196–3202.

(18) Melenkivitz, R.; Mindiola, D. J.; Hillhouse, G. L. *J. Am. Chem. Soc.* **2002**, *125*, 3846–3847.

(19) (a) Garcia, M. E.; Riera, V.; Ruiz, M. A.; Saez, D.; Vaissermann, J.; Jeffery, J. C. *J. Am. Chem. Soc.* **2002**, *124*, 14304–14305. (b) Alvarez, C. M.; Alvarez, M. A.; Garcia, M. E.; Gonzalez, R.; Ruiz, M. A.; Hamidov, H.; Jeffery, J. C. *Organometallics* **2005**, *24*, 5503–5505. (c) Graham, T. W.; Udachin, K. A.; Carty, A. J. *Chem. Commun.* **2005**, 4441–4443.

(20) Ehlers, A. W.; Baerends, E. J.; Lammertsma, K. *J. Am. Chem. Soc.* **2002**, *124*, 2831–2838.

(21) (a) Fermin, M. C.; Stephan, D. *J. Am. Chem. Soc.* **1995**, *117*, 12645–12646. (b) Zhao, G.; Basuli, F.; Kilgore, U. J.; Fan, H.; Aneetha, H.; Huffman, J. C.; Wu, G.; Mindiola, D. J. *J. Am. Chem. Soc.* **2006**, *128*, 13575–13585.

(22) (a) Mathey, F.; Tran Huy, N. H.; Marinetti, A. *Helv. Chim. Acta* **2001**, *84*, 2938–2957. (b) Lammertsma, K.; Vlaar, M. J. M. *Eur. J. Org. Chem.* **2002**, 1127–1138.

(23) Waterman, R.; Hillhouse, G. L. *J. Am. Chem. Soc.* **2003**, *125*, 13350–13351.

(24) Shah, S.; Protasiewicz, J. D. *Coord. Chem. Rev.* **2000**, *210*, 181–201.

(25) Goumans, T. P.; Ehlers, A. W.; Lammertsma, K. *J. Organomet. Chem.* **2005**, *690*, 5517–5524.

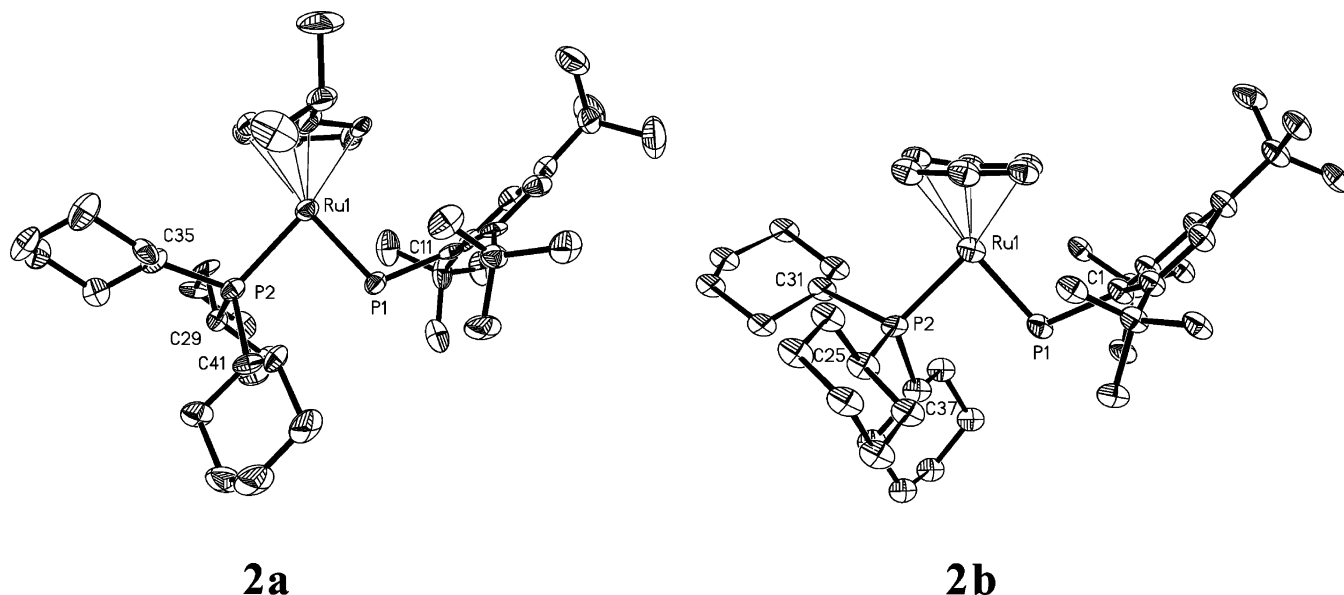
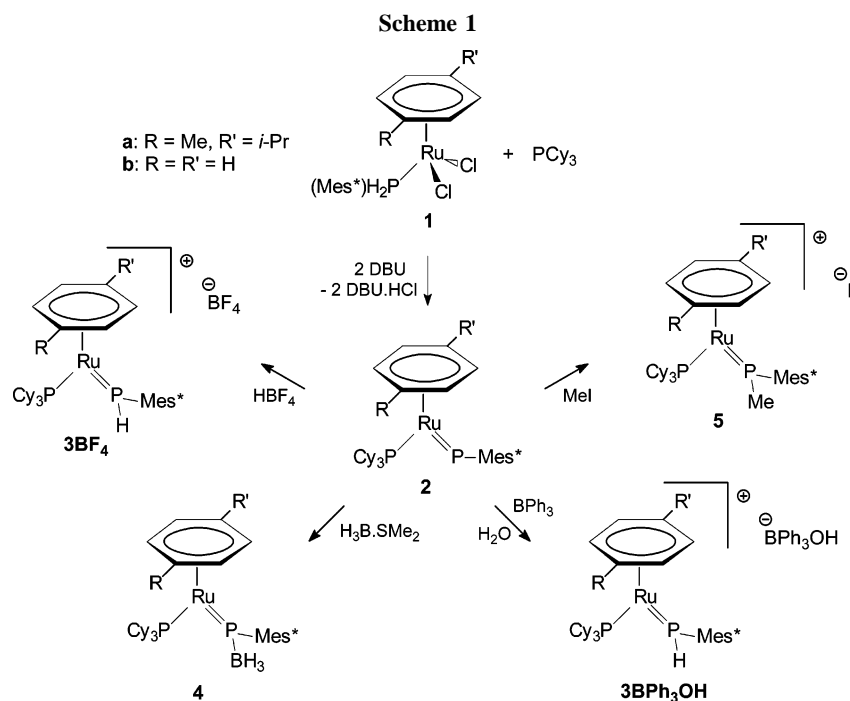


Figure 1. Molecular structure of complexes **2a** and **2b** (50% probability level for the thermal ellipsoids). All H atoms have been omitted for clarity. Selected metrical parameters (Å) and angles (deg): For **2a**: Ru1–P1 2.205(3); Ru–P2 2.386(4); P1–C11 1.843(14); Ru1–centroid(arene) 1.766; P1–Ru1–P2 85.98(14); Ru1–P1–C11 110.5(4). For **2b**: Ru1–P1 2.237(7); Ru1–P2 2.389(7); P1–C1 1.91(2); Ru1–centroid(arene) 1.778; P1–Ru1–P2 86.7(3); Ru1–P1–C1 107.6(8).



Reactivity Studies. The philicity of terminal phosphinidene complexes has been shown to depend essentially on the electronic properties of the ligands.²⁰ The electron-rich fragment (η^6 -Ar)(PCy₃)Ru is expected to induce a significant electronic density flow from the transition metal on the phosphinidene phosphorus and, thus, to enhance nucleophilicity of the phosphinidene ligand. Consistently, the nucleophilicity of the phosphorus atom in **2** is illustrated by its reactivity toward electrophilic reagents.

Reactions with Electrophiles. First, we examined the reactivity of **2** toward Brønsted acids (Scheme 1). Protonation of the phosphinidene atom is readily achieved. However, according to the nucleophilicity of the anion, different complexes are obtained. Reaction with HCl results in the instantaneous formation of (η^6 -Ar)(PCy₃)RuCl₂ (**1**) with the release of PH₂-

Mes*. Treatment of a solution **2** with the acid HBF₄ incorporating the non-nucleophilic anion BF₄⁻ leads to a rapid color change from dark green to purple with formation of the new cationic complexes [(η^6 -Ar)(PCy₃)Ru(PHMes*)]BF₄ (**3aBF₄**, Ar = *p*-cymene; **3bBF₄**, Ar = benzene) in high yields (Scheme 1).

The discrepancy between the reactivity of **2** with HCl and HBF₄ is reminiscent of the somewhat related imido complex (PMe₃)₂ReMe₃(NPh): reaction with HBF₄ led to protonation, while in the case of CH₃COOH a unidentate coordination mode was characterized for acetate.²⁸ These results can be attributed to the relative nucleophilicity of the anions: The presence of **3BF₄** is evident from their ³¹P NMR spectra, which exhibit a

signal assigned to the phosphonium ligand PHMe^{*} at δ 174 ($^1J(\text{P}, \text{H}) = 336$ Hz, $^2J(\text{P}, \text{P}) = 84$ Hz) for **3aBF₄** and at δ 191 ($^1J(\text{P}, \text{H}) = 343$ Hz, $^2J(\text{P}, \text{P}) = 84$ Hz) for **3bBF₄**. Of interest is that these ^{31}P chemical shifts are lower than the values typically found (200–320 ppm) for phosphonium resonances presumably because of the strong donating properties of the ruthenium fragment.²⁹ The ^1H NMR spectra display a resonance at δ 8.86 for **3aBF₄** and δ 9.00 for **3bBF₄** characteristic of the acidic proton of the PHMe^{*} moiety, suggesting the presence of a non-negligible partial positive charge on the phosphorus atom. Other signals are slightly shifted downfield from the corresponding resonances of **2**. Interestingly, to the best of our knowledge, **3aBF₄** and **3bBF₄** are the first P–H-functionalized cationic phosphonium complexes. Despite renewed interest in the phosphonium group as a strong π -acidic ligand in the context of the preparation of electrophilic late transition metal catalysts,³⁰ the range of phosphonium ligands in cationic complexes remains indeed confined quasi-exclusively to diamino, aminoalkoxy, or dialkoxy phosphonium moieties.²⁹ Stabilization of hydrogen-substituted phosphonium and more generally phosphonium ligands bearing weakly π - and σ -donating substituents (for instance aryl or alkyl) represents a true synthetic challenge. [(CO)₄Fe{P(Fc)₂}]AlCl₄ (Fc = ferrocenyl) is the only example for which no N- or O-based substituent (i.e., strongly π -donating and σ -withdrawing fragments) is borne by the two-coordinate phosphorus cation.³¹ However, it could not be characterized using X-ray diffraction techniques. In this case, delocalization on the ferrocenyl substituent is invoked to allow stabilization. Concerning **3BF₄**, the unprecedented stabilization of a phosphonium ligand bearing a hydrogen substituent can be assigned to the powerful electron-rich nature of the fragment ($\eta^6\text{-Ar}$)-(PCy₃)Ru. The decisive factor is, indeed, the π -basicity of the transition metal fragment.²⁹ Computational studies support that stabilization results predominantly from transition metal π -back-donation and as a minor component from π -donation from a phosphorus substituent.²⁹

Single crystals of **3aBF₄** were grown from a toluene solution at -25 °C. The molecular representation is depicted in Figure 2 and confirmed the formulation deduced from NMR consideration. To date, a very limited number of phosphonium complexes have been structurally characterized.²⁹

Similarly to what was observed in the previously reported X-ray diffraction molecular structures, the M–P(phosphonium) bond is substantially shorter (2.173(9) Å) than the M–P dative bond (2.394(8) Å).^{29a} This result is consistent with double-bond character as evidenced with the similar ruthenium–phosphinidene distance found in **2a**. However, all structurally characterized cationic phosphonium complexes involve an amino or alkoxy substituent on the phosphorus atom, and thus, this prevents further relevant comparison. The metrical parameters of the fragment ($\eta^6\text{-Ar}$)-(PCy₃)Ru of **3aBF₄** are very similar to those of **2a** and **2b**, but the protonation of the phosphinidene ligand results in noteworthy modifications of the P–Ru–P and Ru–P–C(Mes^{*}) angles, which increase significantly (91.0(3)° and 132.2(10)°). The latter value compares well to that observed

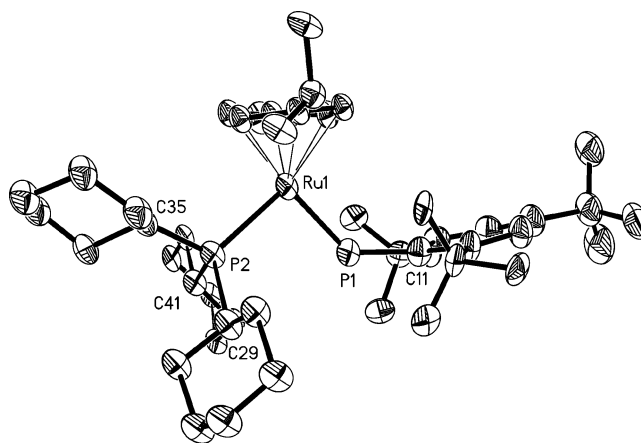


Figure 2. Molecular structure of complex **3aBF₄·C₇H₈** (50% probability level for the thermal ellipsoids). All H atoms, the anion, and the solvent molecule (toluene) have been omitted for clarity. Selected metrical parameters (Å) and angles (deg): Ru1–P1 2.173(9); Ru1–P2 2.394(8); P1–C11 1.79(3); Ru1–centroid(arene) 1.743; P1–Ru1–P2 91.0(3); Ru1–P1–C11 132.2(10).

in the somewhat related phosphido complex ($\eta^5\text{-Cp}'$)(PMe₃)₂-Mo(PHMe^{*}) (Cp' = C₅EtMe₄, Mo–P–C(Mes^{*}) = 133.0(3)°).³²

The lone pair of the phosphorus atom of the phosphinidene ligand remains also accessible to electrophilic alkylating reagents and Lewis acids. Treatment of **2** with an excess of BH₃·SMe₂ gives the expected adducts ($\eta^6\text{-Ar}$)(PCy₃)Ru[P(BH₃)Mes^{*}] (**4a**, Ar = *p*-cymene; **4b**, Ar = benzene) (Scheme 1), which were characterized spectroscopically. These borane adducts decomposed on attempted recrystallization, and satisfactory elemental analysis could not be obtained. Although no ^{11}B – ^{31}P coupling is observed, the ^{31}P NMR spectrum shows some line broadening and the PMe^{*} chemical shift changes significantly on complexation (from 813 to 506 ppm for **4a** and from 819 to 521 ppm for **4b**). For comparison, on formation of the adduct PH₂-Mes^{*}·BH₃, the ^{31}P NMR signal moves from δ –130 to –62.²⁷ Additionally, the ^{11}B NMR spectra display resonances in the expected range for a tetracoordinated boron atom (at δ 18.3 for **4a** and **4b**), consistent with a rehybridization at boron.

Replacing BH₃ by BPh₃ leads to interesting results. In a first stage, no reaction is observed, the size of the borane BPh₃ disfavoring presumably its coordination. However, in the presence of water, the color of the solution changes to purple. In the ^1H , ^{31}P , and ^{13}C NMR spectra, very similar resonances to those of **3BF₄** were observed and assigned to [($\eta^6\text{-Ar}$)-(PCy₃)Ru(PHMe^{*})]BPh₃OH (**3BPh₃OH**) (Scheme 1). ^{11}B NMR resonances for **3aBPh₃OH** and **3bBPh₃OH** allow unequivocal identification of a tetracoordinated boron atom. Studies on properties of boranes and in particular of B(C₆F₅)₃ have focused much interest and have shown that water adducts may be regarded as strong Brønsted acid.³³ The pK_a for the complex (C₆F₅)₃B·OH₂ is estimated to be 8.4 in acetonitrile. Such a value indicates that (C₆F₅)₃B·OH₂ and HCl possess comparable Brønsted acidity. However, there is, to the best of our knowledge, no report concerning direct or indirect observation of the adduct Ph₃B·OH₂, which is assumed to be involved in the formation of **3BPh₃OH**. Interestingly, a significant difference is observed for the ^1H , ^{31}P , and ^{13}C NMR arene signals of **3aBPh₃OH** (and **3bBPh₃OH**) compared to those of **3aBF₄** (and **3bBF₄**). This result suggests some sort of ion-

(28) Chiu, K. W.; Wong, W. K.; Wilkinson, G. *Polyhedron* **1982**, *1*, 31–36.

(29) (a) Nakazawa, H. *Adv. Organomet. Chem.* **2004**, *50*, 108–143. (b) Gudat, D. *Eur. J. Inorg. Chem.* **1998**, 1087–1094.

(30) (a) Hardman, N. J.; Abrams, M. B.; Pribisko, M. A.; Gilbert, T. M.; Martin, R. L.; Kubas, G. J.; Baker, R. T. *Angew. Chem., Int. Ed.* **2004**, *43*, 1955–1958. (b) Spinney, H. A.; Yap, G. P. A.; Korobkov, I.; DiLabio, G.; Richeson, D. S. *Organometallics* **2006**, *25*, 3541–3543.

(31) Baxter, S. G.; Collins, R. L.; Cowley, A. H.; Sena, S. F. *J. Am. Chem. Soc.* **1981**, *103*, 714–715.

(32) Hey-Hawkins, E.; Fromm, K. *Polyhedron* **1995**, *14*, 2825–2834.

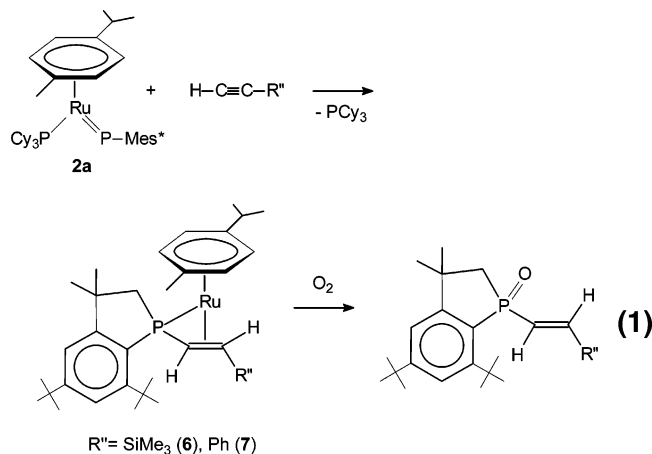
(33) Bergquist, C.; Bridgewater, B. M.; Harlan, C. J.; Norton, J. R.; Friesner, R. A.; Parkin, G. *J. Am. Chem. Soc.* **2000**, *122*, 10581–10590.

pairing interactions involving anion and η^6 -Ar ligands. However, the exact origin of these phenomena remains to be clarified.

The reactivity of **2a** and **2b** toward electrophilic alkylating reagents such as organic iodides was also examined. Treatment of **2** with 1 equiv of methyl iodide leads to the alkylation at the phosphinidene center and yields the phosphonium complexes $[(\eta^6\text{-Ar})(\text{PCy}_3)\text{Ru}(\text{PMeMes}^*)]\text{I}$ (**5a**, Ar = *p*-cymene; **5b**, Ar = benzene), which can be isolated as purple solids (Scheme 1). This structural formulation is based on the ^1H , ^{13}C , and ^{31}P NMR spectra. The ^{31}P NMR spectra display doublets of quadruplets at δ 240 ($^2J_{\text{PH}} = 9.7$ Hz; $^2J_{\text{PP}} = 82.1$ Hz) and 248 ($^2J_{\text{PH}} = 10.2$ Hz; $^2J_{\text{PP}} = 76.3$ Hz) for the phosphonium ligand P(Me)(Mes *) in **5a** and **5b**, respectively. Accordingly, in the ^1H NMR spectra, the methyl signals appear as doublets (2.13 ppm, $^2J_{\text{PH}} = 9.7$ Hz for **5a** and 2.21 ppm, $^2J_{\text{PH}} = 10.2$ Hz for **5b**) arising from the coupling with the phosphorus nucleus. In addition, the NMR data of **5** compare well to those of complexes **3** and are consistent with the formation of cationic complexes with a phosphonium ligand.

However, interestingly the *p*-cymene ligand in **5a** no longer exhibits fluxional behavior anymore, as evidenced by the ^1H NMR spectrum, which shows for the aryl protons of the *p*-cymene ligand three resonances in a 2:1:1 ratio, the last two being significantly shifted upfield relative to those of **3a $^+$. Such a behavior had been previously observed in the related metaphosphonate complex $(\eta^6\text{-}p\text{-cymene})(\text{PCy}_3)\text{Ru}((\eta^2\text{-OPOMes}^*))^{26}$ and for half-sandwich complexes exposed to the magnetic anisotropy cone of the phenyl substituent (known as the “ β -phenyl effect”). 34 Consistently, the proximity between *p*-cymene and Mes * moieties results also in restricted rotation about the P–C(Mes *) bond, as evidenced by the presence of two Mes * aryl signals in addition to two *o*-Me resonances. This result is attributed to the higher steric congestion around the ruthenium atom in **2a** compared to that in **2b**. This prompted us to study the reactivity of **2** with the larger alkyl reagent isopropyl iodide. However, no reaction was observed, confirming that if there is a difference in terms of steric hindrance; both complexes remain highly encumbered, preventing in this case the electrophilic attack.**

Reactions with Alkynes: Mechanistic Studies. Despite the electron-rich nature of the ruthenium fragment and the nucleophilicity of the phosphinidene ligand, **2a** reacts instantaneously with alkynes ($\text{Me}_3\text{SiC}\equiv\text{CH}$ and $\text{PhC}\equiv\text{CH}$) to afford the allylphosphaindane complexes **6** and **7** (eq 1).



The formation of **6** and **7** and the release of PCy_3 are evident from the NMR data. In the ^1H and ^{13}C NMR spectra of **6** and

7 signals corresponding to two nonequivalent *t*-Bu groups, four Me groups, and a new CH_2 moiety indicate unambiguously the formation of a coordinated vinylphosphine fragment. 35 Additionally, the presence of vinylic proton signals at $\delta \sim 2.4$ and 3.4 coupled with a phosphorus nucleus clearly shows the formation of a coordinated vinylphosphine fragment. These assignments are in agreement with those of an analogous complex that has been recently fully characterized and showed similar NMR resonances. 15 Furthermore, **6** and **7** have been prepared separately using the method described by Lammerstma et al., that is, by reacting $(\eta^6\text{-}p\text{-cymene})(\text{PH}_2\text{Mes}^*)\text{RuCl}_2$ with 2 equiv of DBU in the presence of the corresponding alkyne. 15

Of interest to note is that the addition of these unsymmetrical alkynes occurs regioselectively with the larger substituent R'' located *trans* to the phosphorus atom. Only one regioisomer is observed by ^1H NMR spectroscopy since the spectrum displays one set of resonances for Ph (or for SiMe_3). Oxidation of **6** allowed formation and crystallization of the oxidized version of the vinylphosphaindane ligand. Despite the poor quality of these crystals, connectivity of atoms was unambiguously established and evidenced the *trans* geometry of the phosphavinyl derivative. 36

This result is consistent with the trend observed for the reaction of zirconocene imido 37 or phosphinidene complexes 38 with alkynes. The regioselectivity has been rationalized in terms of steric repulsion between the substituent of the phosphinidene (or imido) group and the ones of the alkyne.

In marked contrast, no reaction occurs with **2b**. Additionally, the high reactivity of **2a** is in total contradiction with the lack of reactivity of the previously reported group 8 and 9 series compounds. 15,16 Such a difference between the chemical behavior of **2a** and **2b** was very surprising, since neither the spectroscopic properties, structural characteristics, nor the preliminary reactivity studies give any insight of potentially different reactivity. This prompted us to study the details of the reaction. The phosphinidene ligand exhibits nucleophilic properties, and thus, the first step is thought to be the coordination of alkyne at the ruthenium center in order to allow the reaction to proceed. The second step of this anticipated mechanism (formation of a metallacycle) is analogous to that described in the case of a related zirconium complex, 39 then followed by an intramolecular C–H insertion of the P atom and subsequent H transfer to yield **6** or **7** (Scheme 2).

Evidently, the key step for the understanding of the specificity of our system is the generation of the complex $(\eta^6\text{-}p\text{-cymene})(\eta^2\text{-HC}\equiv\text{CR}'')\text{Ru}(\text{PMe}^*)$, which has, thus, focused our interest. In the two limiting cases, complexation of alkyne could occur according to an associative or a dissociative mechanism. In the latter case, phosphine dissociation to generate a 16-electron intermediate, $(\eta^6\text{-}p\text{-cymene})\text{Ru}(\text{PMe}^*)$, is an appealing hypothesis for synthetic outcomes since it would provide an entry to the chemistry of an unsaturated phosphinidene species related to the valuable $\text{Cp}_2(\text{PMe}_3)\text{Zr}(\text{PMe}^*)$ complex. Involvement of $(\eta^6\text{-Ar})\text{Ru}(\text{PMe}^*)$ has also been proposed to account for the formation of several complexes connected to phosphinidene

(35) Aitken, R. A.; Clasper, P. N.; Wilson, N. J. *Tetrahedron Lett.* **1999**, 40, 5271–5274.

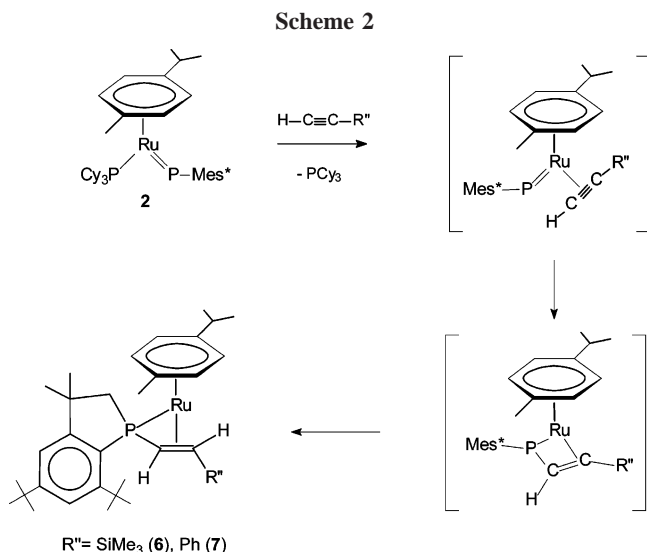
(36) Because a single crystal was of low quality, the details of the structural parameters could not be discussed, but the regiochemistry of the olefin moiety was determined to be the *E*-configuration.

(37) Baranger, A. M.; Walsh, P. J.; Bergman, R. G. *J. Am. Chem. Soc.* **1993**, 115, 2753–2763.

(38) Breen, T. L.; Stephan, D. W. *Organometallics* **1996**, 15, 5729–5737.

(39) Breen, T. L.; Stephan, D. W. *J. Am. Chem. Soc.* **1996**, 118, 4204–4205.

(34) Brunner, H.; Zwack, T.; Zabel, M.; Beck, W.; Böhm, A. *Organometallics* **2003**, 22, 1741–1750.



species.¹⁵ However, a recent computational study on the related group 9 metals phosphinidene complexes of general formula $\text{Cp}^*(\text{PPh}_3)\text{M}(\text{PMes}^*)$ ($\text{M} = \text{Co}, \text{Rh}, \text{Ir}$) showed a high dissociation energy of the stabilizing phosphine ligand.¹⁶ Additionally, an associative pathway should not be excluded since the freeing of a coordination site may also be achieved through ligand-induced ring slippage of η^6 - to η^4 -arene, as previously reported for the reaction of phosphine, phosphite, or isonitrile with a related ruthenium-naphthalene complex.⁴⁰ Finally, migration of a metal fragment off the arene centroid and more generally arene exchange have been shown to be facilitated for arene- ML_2 complexes.⁴¹

Preliminary studies proved that it was difficult to investigate mechanistic details in solution since none of the putative ruthenium intermediate could be observed by spectroscopic means. Consequently, we undertook a detailed kinetic study on phosphine complexation as a model for the alkyne coordination (Scheme 3).

This approach was successfully exploited for a phosphine/olefin substitution study on Grubbs' ruthenium-based olefin metathesis catalysts.⁴² However, the rate of exchange between free phosphines and PCy_3 is insufficient to support spin-saturation labeling experiments as kinetic probes. Therefore, the concentration of the exchange products was monitored with time by ^1H NMR. This substitution reaction is reversible since the same product distribution (K) can also be established from the reaction of $(\eta^6\text{-}p\text{-cymene})(\text{PPh}_3)\text{Ru}(\text{PMes}^*)$ (**8**) with PCy_3 .

A numerical approach was used to treat the kinetic curves. The two models (see Supporting Information) corresponding

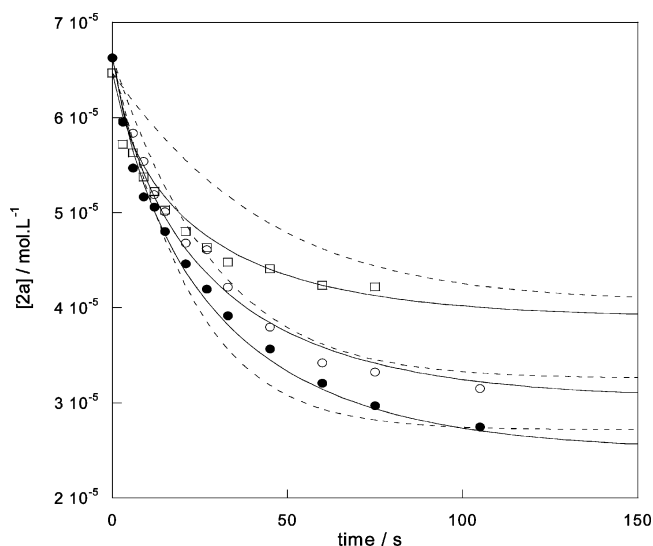


Figure 3. Plot of $[2a]$ versus time at different concentrations of PPh_3 (\square 1 equiv, \circ 2 equiv, \bullet 3 equiv). Solid line: best fit obtained for the three curves simultaneously using the dissociative model. Dotted line: best fit using the associative model.

to the two proposed pathways were used to reproduce the experimental data. When only one experiment is presented to each model, the quality of the fitting obtained is equivalent and does not allow a choice between the two mechanisms. This problem was resolved by fitting simultaneously three experiments involving increasing concentrations of PPh_3 (1, 2, and 3 equiv). The result is in this case clearly in favor of the dissociative pathway (Figure 3).

The parameters extracted from the fitting procedure are (i) the dissociation rate of PCy_3 ($k_1 = 3.3 \times 10^{-2} \text{ s}^{-1}$) and (ii) that of PPh_3 ($k_{-2} = 8.5 \times 10^{-3} \text{ mol}^{-1}\cdot\text{L}\cdot\text{s}$); (iii) without further information on the intermediate concentration the constants k_{-1} and k_2 cannot be reached, but their ratio can ($k_{-1}/k_2 = 9$). These results show that rate constants involving PCy_3 are larger than those of PPh_3 : dissociation of PCy_3 from $(\eta^6\text{-}p\text{-cymene})(\text{PCy}_3)\text{Ru}(\text{PMes}^*)$ (**2a**) is faster than that of PPh_3 from $(\eta^6\text{-}p\text{-cymene})(\text{PPh}_3)\text{Ru}(\text{PMes}^*)$ (**8**), and trapping of PCy_3 by the intermediate **A** is also quicker than that of PPh_3 . This result was unanticipated since a less electron-donating phosphine is generally expected to be more labile.⁴² Addressing the relative importance of steric and electronic factors for tertiary phosphine ligands has attracted much recent attention due to their ubiquitous involvement in organometallic chemistry. In order to gain insight into the relative influence of these factors, experiments were conducted for a series of phosphines. For this study, the kinetic curves

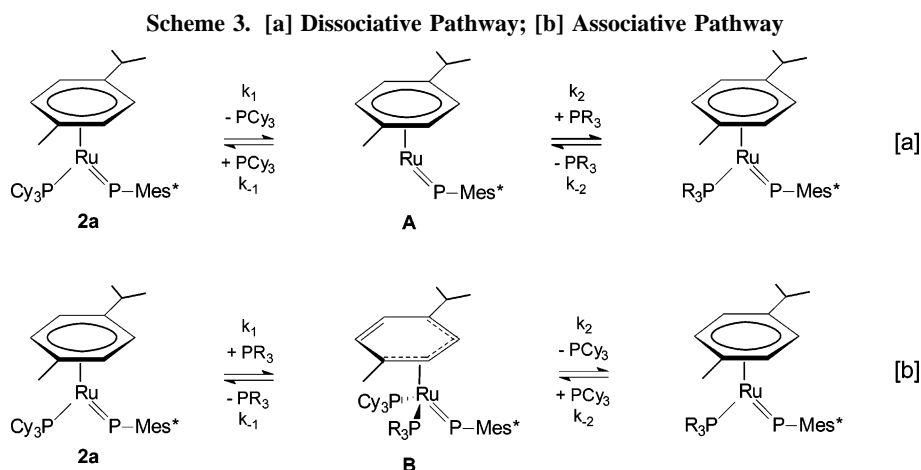


Table 1. Kinetic Parameters Extracted from Phosphine Exchange Reaction

entry	PR ₃	K	k_{-1}/k_2 coord	k_1/k_{-2} dissos	k_{-2} (mol ⁻¹ ·L·s)	pK _a ^a	ν_{CO} ^b (cm ⁻¹)	θ^c (deg)
1	P(NC ₄ H ₄) ₃	78	0.9	72.6	4.60×10^{-4}	n.d.	2090.4 ^d	145 ^d
2	P(<i>p</i> -ClC ₆ H ₄) ₃	0.85	1.6	1.4	2.42×10^{-2}	1.03	2072.8	145
3	PPh ₃	0.44	9.0	3.9	8.51×10^{-3}	2.73	2068.9	145
4	P(<i>p</i> -MeOC ₆ H ₄) ₃	0.24	13.1	3.2	1.06×10^{-2}	4.59	2066.1	145
5	P(<i>m</i> -MeC ₆ H ₄) ₃	0.86	6.8	7.8	4.26×10^{-3}	3.30	2067.2	165
6	P(<i>o</i> -MeC ₆ H ₄) ₃	0				3.08	2066.6	194
7	P(<i>o</i> -MeOC ₆ H ₄) ₃	0				~8.8 ^e	n.d.	205 ^f

^a pK_a of the corresponding conjugate acid.⁴³ ^b ν_{CO} : carbonyl stretching frequency in the corresponding Ni(CO)₃L complex in CH₂Cl₂.⁴³ ^c Tolman cone angle.⁴³ ^d Electronic and steric properties are discussed in ref 44. ^e Electronic properties of P(*o*-MeOC₆H₄)₃ were found to be comparable to those of P(*i*-Pr)₃.^{45a} ^f Reference 45b.

were treated with the dissociative model, the values of k_1 and k_{-1} were fixed to those obtained previously, and k_2 and k_{-2} were provided by fitting. Rate constants of substitution reactions and steric (Tolman cone angle) and electronic characteristics⁴³ are gathered in Table 1. Considering isosteric phosphines (P(NC₄H₄)₃,⁴⁴ P(*p*-ClC₆H₄)₃, PPh₃, P(*p*-MeOC₆H₄)₃, entries 1 to 4), the less basic the phosphine, the more the equilibrium is driven toward the formation of the new complexes (η^6 -*p*-cymene)(PR₃)Ru(PMes*) (K increases). On the other hand, examination of the ratio between coordination rate constants (k_{-1}/k_2) establishes a clear trend: the donor properties of PR₃ slow down its trapping by **A**. As a consequence, changing the phosphine from P(NC₄H₄)₃ to P(*p*-MeOC₆H₄)₃ leads indeed to an approximately 15-fold decrease in the coordination rate. The effect of electronic properties on the dissociation rate constants (k_1/k_{-2}) looks less obvious to rationalize in the cases of the three arylphosphines (entries 2–4) since the variations are relatively weak. A similar observation was made by Grubbs et al. (during the study of phosphine dissociation in ruthenium olefin metathesis catalysts), who stressed the point that no linear correlation between phosphine pK_a and its dissociation rate constant exists.⁴² However, it is interesting to note that in the case of P(NC₄H₄)₃ the dissociation is significantly disfavored (20-fold, entry 1).

Concerning the influence of steric effects, the phosphine PCy₃ in **2a** exchanges only with smaller phosphines, evidencing the dominant role of the congestion of the added phosphine. This is in particular illustrated by the absence of reaction of **2a** with P(*o*-MeC₆H₄)₃ or P(*o*-MeOC₆H₄)₃,⁴⁵ although their electronic properties should promote coordination (because they are less basic) and disfavor decoordination.⁴⁶ Interestingly, this positive influence of a large phosphine was unexpected since the reactivity of Cp*(PR₃)Rh(PMes*) has been shown to increase by reducing the size of its stabilizing ligand PR₃.¹⁶

Two important ligand effects in this system involve an acceleration of the critical step of phosphine dissociation: the donating and the hindering characteristics of the PR₃ ligand. In other words, the presence of a strongly π -acidic phosphine

P(NC₄H₄)₃ led to an important stabilization of the phosphinidene complex **12**. As an illustration, only 10% of conversion of phenylacetylene into **7** is observed when reacting **12** at 50 °C for 3 days. The inertness of **12** is consistent with a DFT study on group 9 transition metal phosphinidene complexes, which stressed a significant increase of the bond dissociation energy of the highly π -acidic carbonyl ligand compared to that of phosphine.¹⁶ However, the dominant effect is unambiguously steric. This result is in perfect agreement with the observation that reaction of alkynes occurs exclusively in the presence of the more hindered arene, which plays the role of reactivity switch.

Conclusion

In summary, ruthenium phosphinidene complexes (η^6 -Ar)-(PCy₃)Ru(PMes*) that differ only in the substituent borne by the arene ligand were prepared and showed dramatically different chemical behavior toward alkynes: introduction of alkyl groups on the arene ligand, i.e., changing the arene ligand from benzene to *p*-cymene, allowed the reaction with alkyne to proceed. A detailed comparative study of the structural and spectroscopic features of both complexes did not allow the identification of the origin of this phenomenon. Reactivity studies of (η^6 -Ar)(PCy₃)Ru(PMes*) with HBF₄ and MeI have afforded unprecedented cationic phosphonium complexes and have provided a first insight for addressing this issue: in the case of [(η^6 -Ar)(PCy₃)Ru(PMeMes*)]I, the free rotation of the Mes* substituent and Ar ligand was stopped only in the case of the more crowded arene ligand, suggesting that alkyl groups of *p*-cymene could be not as innocent as initially anticipated. Careful examination of the mechanism of reaction of phosphinidene complexes with alkyne and in particular of the first step (phosphine dissociation) brought evidence for the involvement of both electronic and steric factors. We have demonstrated that in contrast with common expectations the lability of the phosphine increased with its donor properties. However, the dominant factor proved to be steric, the specificity of (η^6 -*p*-cymene)(PCy₃)Ru(PMes*) being directly related to the critical PCy₃ dissociation step, which occurs only when the arene is *p*-cymene. Thus, the reactivity arises from the repulsion of the sterically demanding phosphine ligand with the alkyl groups of the arene ligand.

Increasing steric congestion about reactive centers is a well-known strategy for kinetic stabilization or for controlling chemo-,⁴⁷ regio-,⁴⁸ or enantioselectivity.⁴⁹ Nevertheless, to the

(40) Bennett, M. A.; Lu, Z.; Wang, X.; Bown, M.; Hockless, D. C. R. *J. Am. Chem. Soc.* **1998**, *120*, 10409–10415.

(41) Muettterties, E. L.; Bleeke, J. R.; Wucherer, E. J.; Albright, T. A. *Chem. Rev.* **1982**, *82*, 499–525.

(42) Sandford, M. S.; Love, J. A.; Grubbs, R. H. *J. Am. Chem. Soc.* **2001**, *123*, 6543–6554.

(43) Tolman, C. A. *Chem. Rev.* **1977**, *77*, 313–348. For PCy₃, the pK_a of the corresponding conjugate acid is 9.7; the carbonyl stretching frequency in the corresponding Ni(CO)₃L complex in CH₂Cl₂ is 2056.4 cm⁻¹, and Tolman cone angle (θ) is 170°.

(44) Moloy, K. G.; Petersen, J. L. *J. Am. Chem. Soc.* **1995**, *117*, 7696–7710.

(45) (a) Pruchnick, F. P.; Smolenski, P.; Wajda-Hermanowicz, K. *J. Organomet. Chem.* **1998**, *570*, 63–69. (b) Suomalainen, P.; Laitinen, R.; Jääskeläinen, S.; Haukka, M.; Pursiainen, J. T.; Pakkanen, T. A. *J. Mol. Catal. A* **2002**, *179*, 93–100.

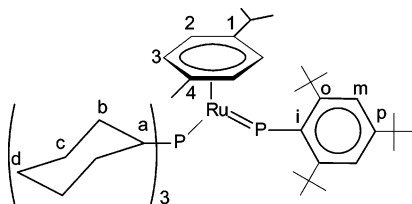
(46) We have checked that the two complexes (η^6 -*p*-cymene)[P(*o*-MeOC₆H₄)₃]Ru(PMes*) and (η^6 -*p*-cymene)[P(*o*-MeC₆H₄)₃]Ru(PMes*) could be prepared separately and, thus, that these phosphines are not too large to prevent their formation.

(47) Ananikov, V. P.; Szilagy, R.; Morokuma, K.; Musaev, D. G. *Organometallics* **2005**, *24*, 1938–1946.

best of our knowledge, it is the first evidence reporting that such a subtle change induces a reactivity switch. This study provides a rare example for which the “catch 22” situation of kinetic stabilization versus reactivity⁴ vanishes: hindering of the large phosphine results on one hand in the stabilization of the metal–phosphinidene bond and, on the other hand, in the enhancement of the elimination rate of the phosphine that enables the coordination of reactants. The reactivity of (η^6 -Ar)-(PCy₃)Ru(PMes*) and of Cp₂(PMe₃)Zr(PMes*) arise, thus, from the same facile dissociation of the stabilizing ligand. In the latter case, the pronounced oxo- and halophilicity of zirconium⁴ has been used elegantly to produce new sophisticated phosphorus-based molecules from carbonyl or dichloride compounds. Concerning (η^6 -Ar)(PCy₃)Ru(PMes*), the functional group tolerance of ruthenium⁵⁰ could also be exploited to complement the scope of these reactions and to open up new perspectives for synthetic applications of these nucleophilic phosphinidene species.

Experimental Section

General Considerations. All reactions were carried out under argon atmosphere using standard Schlenk techniques. Solvents were dried and distilled according to standard procedures and degassed prior to use. All reagents were purchased from Aldrich and were used without further purification. NMR spectra were recorded in C₆D₆ on Bruker AC 200 or ARX 400 instruments. Infrared spectra were recorded with a Perkin-Elmer 1600 FT spectrometer. Elemental analyses were done by the Centre de Microanalyses de l'École Nationale Supérieure de Chimie de Toulouse. ¹H and ¹³C{¹H} NMR assignments were confirmed by ¹H COSY, HSQC (¹H–¹³C), and HMQC (¹H–¹³C) experiments. (η^6 -*p*-Cymene)(PCy₃)RuCl₂, (η^6 -benzene)(PCy₃)RuCl₂, (η^6 -*p*-cymene)(PPh₃)RuCl₂, (η^6 -*p*-cymene)-[P(*p*-ClC₆H₄)₃]RuCl₂, (η^6 -*p*-cymene)[P(*p*-MeC₆H₄)₃]RuCl₂, (η^6 -*p*-cymene)[P(*p*-MeOC₆H₄)₃]RuCl₂, (η^6 -*p*-cymene)[P(NC₄H₄)₃]RuCl₂, (η^6 -*p*-cymene)[P(*m*-MeC₆H₄)₃]RuCl₂, and (η^6 -*p*-cymene)[P(*o*-MeOC₆H₄)₃]RuCl₂ were prepared according to literature procedures.⁵¹ Atom labeling used in the NMR assignments of **2–13** is given below (for example **2a**):



(η^6 -*p*-Cymene)(PCy₃)Ru(PMes*) (**2a**). To a red slurry of (η^6 -*p*-cymene)(PH₂Mes*)RuCl₂ (0.601 g; 1.03 mmol) and PCy₃ (0.274 g; 0.98 mmol) in toluene (10 mL) was added DBU (0.29 mL; 1.97 mmol). The mixture was stirred for 1 h at room temperature to afford a dark green solution. The toluene was removed *in vacuo* and the dark green solid then extracted with pentane (10 mL) and filtered to remove DBU·HCl. Removal of the pentane to a minimal volume and cooling to –25 °C gave 0.780 g of a crystalline solid in 80% yield. Mp: 168 °C dec. ³¹P NMR (81.0 MHz): δ 35.27 (d,

²J_{PP} = 15.3 Hz, PCy₃); 812.94 (d, ²J_{PP} = 15.3 Hz, PMes*). ¹H NMR (400.1 MHz): δ 1.05 (d, ³J_{HH} = 6.6 Hz, 6H, C₁–CH–(CH₃)₂); 1.31 (m, 12H, C₆H₂); 1.57 (s, 9H, C_p–C–(CH₃)₃); 1.74 (s, 18H, C_o–C–(CH₃)₃); 1.76 (s, 3H, C₄–CH₃); 1.93 (m, 6H, C_dH₂); 2.11 (m, 12H, C_bH₂); 2.56 (m, 4H, C₁–CH–(CH₃)₂ and C_aH); 4.71 (AB, ³J_{HH} = 5.9 Hz, 2H, C₃H); 4.79 (AB, ³J_{HH} = 5.9 Hz, 2H, C₂H); 7.56 (d, ⁴J_{HP} = 3.9 Hz, 2H, C_mH). ¹³C{¹H} NMR (100.6 MHz): δ 18.74 (C₄–CH₃); 24.42 (C₁–CH–(CH₃)₂); 27.37 (C_d); 28.35 (d, ³J_{CP} = 9.2 Hz, C_c); 30.33 (C_b); 31.29 (C₁–CH–(CH₃)₂); 31.95 (C_p–C–(CH₃)₃); 32.80 (C_o–C–(CH₃)₃); 34.93 (C_p–C–(CH₃)₃); 36.84 (C_a); 38.77 (C_o–C–(CH₃)₃); 81.46 (C₃); 86.07 (C₂); 89.58 (C₄); 103.53 (C₁); 119.09 (C_m); 145.35 (C_p); 145.99 (C_o); 176.52 (C_i determined using 2D NMR experiments). Anal. Calcd for C₄₆H₇₆P₂Ru: C, 69.75; H, 9.67. Found: C, 69.65; H, 9.47.

(η^6 -Benzene)(PCy₃)Ru(PMes*) (**2b**). A similar procedure to that described for **2a** was used. (η^6 -Benzene)(PH₂Mes*)RuCl₂ (0.321 g; 0.61 mmol) and PCy₃ (0.164 g; 0.59 mmol) gave **2b** as a green solid (0.187 g, 42%). Crystallization from pentane at –25 °C gave green crystals suitable for X-ray analysis. Mp: 180 °C dec. ³¹P NMR (81.0 MHz): δ 38.09 (d, ²J_{PP} = 7.6 Hz, PCy₃); 819.06 (d, ²J_{PP} = 7.6 Hz, PMes*). ¹H NMR (200.1 MHz): δ 1.31 (m, 12H, C₆H₂); 1.57 (s, 9H, C_p–C–(CH₃)₃); 1.69 (s, 18H, C_o–C–(CH₃)₃); 1.83 (m, 12H, C_bH₂); 2.07 (m, 6H, C_dH₂); 2.58 (m, 3H, C_aH); 4.69 (s, 6H, CH_{benzene}); 7.56 (s, 2H, C_mH). ¹³C{¹H} NMR (50.3 MHz): δ 27.41 (C_d); 28.32 (d, ³J_{CP} = 10.2 Hz, C_c); 30.46 (C_b); 31.88 (C_p–C–(CH₃)₃); 32.35 (C_o–C–(CH₃)₃); 34.93 (C_p–C–(CH₃)₃); 36.26 (dd, ¹J_{CP} = 19.4 Hz, ³J_{CP} = 5.5 Hz, C_a); 38.14 (C_o–C–(CH₃)₃); 81.90 (C_{benzene}); 119.69 (C_m); 145.69 (C_p); 145.95 (C_o). Anal. Calcd for C₄₂H₆₈P₂Ru: C, 68.54; H, 9.31. Found: C, 67.89; H, 9.05.

(η^6 -*p*-Cymene)(PCy₃)Ru(PHMes*)BF₄ (**3aBF₄**). To a green solution of **2a** (0.135 g, 0.17 mmol) in toluene (5 mL) was added 0.18 mmol of HBF₄ (54 wt % in Et₂O). The solution turned immediately to violet, and the mixture was stirred for 10 min at room temperature. The volatiles were removed *in vacuo*, leaving a violet residue. Trituration with pentane afforded pure **3aBF₄** as a violet powder (0.131 g, 88%). Crystallization from toluene at –25 °C gave green crystals suitable for X-ray analysis. Mp: 117 °C. ³¹P NMR (81.0 MHz): δ 45.39 (dd, ²J_{PP} = 83.9 Hz, ³J_{PH} = 18.9 Hz, PCy₃); 173.94 (dd, ¹J_{PH} = 335.7 Hz, ²J_{PP} = 83.9 Hz, PHMes*). ¹H NMR (400.1 MHz): δ 1.07 (d, ³J_{HH} = 6.5 Hz, 6H, C₁–CH–(CH₃)₂); 1.36 (m, 12H, C₆H₂); 1.46 (s, 9H, C_p–C–(CH₃)₃); 1.51 (s, 18H, C_o–C–(CH₃)₃); 1.76 (s, 3H, C₄–CH₃); 1.95 (m, 6H, C_dH₂); 2.25 (m, 12H, C_bH₂); 2.77 (m, 3H, C_aH); 3.03 (m, 1H, C₁–CH–(CH₃)₂); 5.32 (AB, ³J_{HH} = 4.7 Hz, 2H, C₃H); 5.79 (AB, ³J_{HH} = 4.7 Hz, 2H, C₂H); 7.61 (s, 2H, C_mH); 8.86 (dd, ¹J_{HP} = 335.7 Hz, ³J_{HP} = 18.9 Hz, PHMes*). ¹³C{¹H} NMR (100.6 MHz): δ 18.00 (C₄–CH₃); 23.74 (C₁–CH–(CH₃)₂); 26.97 (C_d); 27.47 (d, ³J_{CP} = 9.2 Hz, C_c); 30.39 (C_b); 31.34 (C_p–C–(CH₃)₃); 31.51 (C₁–CH–(CH₃)₂); 32.70 (C_o–C–(CH₃)₃); 33.71 (d, ¹J_{CP} = 7.4 Hz, C_a); 35.46 (C_p–C–(CH₃)₃); 38.88 (C_o–C–(CH₃)₃); 84.87 (C₃); 89.45 (C₂); 100.31 (C₄); 113.03 (C₁); 122.81 (d, ³J_{CP} = 8.3 Hz, C_m); 152.70 (C_o); 153.00 (C_p); 166.03 (C_i). ¹⁹F NMR (188.3 MHz): δ –73.40 (s). ¹¹B NMR (96.3 MHz): δ –0.12 (br s). Anal. Calcd for C₄₆H₇₇BF₄P₂Ru: C, 62.79; H, 8.82. Found: C, 62.31; H, 8.58.

(η^6 -Benzene)(PCy₃)Ru(PHMes*)BF₄ (**3bBF₄**). A similar procedure to that described for **3aBF₄** was used. **2b** (0.125 g; 0.17 mmol) and HBF₄ (0.18 mmol, 54 wt % in Et₂O) gave **3bBF₄** as a violet solid (0.113 g, 81%). Mp: 126 °C. ³¹P NMR (81.0 MHz): δ 48.31 (dd, ²J_{PP} = 83.9 Hz, ³J_{PH} = 16.7 Hz, PCy₃); 190.93 (dd, ¹J_{PH} = 343.3 Hz, ²J_{PP} = 83.9 Hz, PHMes*). ¹H NMR (300.1 MHz): δ 1.41 (m, 12H, C₆H₂); 1.44 (s, 9H, C_p–C–(CH₃)₃); 1.52 (s, 18H, C_o–C–(CH₃)₃); 1.82 (m, 6H, C_dH₂); 2.02 (m, 12H, C_bH₂); 2.53 (m, 3H, C_aH); 5.30 (s, 6H, CH_{benzene}); 7.53 (s, 2H, C_mH); 9.00 (dd, ¹J_{HP} = 343.3 Hz, ³J_{HP} = 16.7 Hz, 1H, PH). ¹³C{¹H} NMR (75.5 MHz): δ 26.56 (C_d); 27.25 (d, ³J_{CP} = 10.5 Hz, C_c); 30.10 (C_b); 31.41 (C_p–C–(CH₃)₃); 32.34 (C_o–C–(CH₃)₃); 33.82 (d, ¹J_{CP} = 7.2 Hz, C_a); 36.45 (C_p–C–(CH₃)₃); 38.27 (C_o–C–(CH₃)₃); 87.06

(48) Bouzbouz, S.; Simmons, R.; Cossy, J. *Org. Lett.* **2004**, *6*, 3465–3467.

(49) Cornejo, A.; Fraile, J. M.; Garcia, J. I.; Gil, M. J.; Martinez-Merino, V.; Mayoral, J. A.; Salvatella, L. *Angew. Chem., Int. Ed.* **2005**, *44*, 458–461.

(50) Trnka, T. M.; Grubbs, R. H. *Acc. Chem. Res.* **2001**, *34*, 18–29.

(51) (a) Martin, M. A. *J. Chem. Soc., Dalton Trans.* **1974**, 233–241. (b) Bennett, M. A.; Matheson, T. W.; Robertson, T. W.; Smith, A. K.; Tucker, P. A. *Inorg. Chem.* **1980**, 1014–1021. (c) Zelonka, R. A.; Baird, M. C. *Can. J. Chem.* **1972**, 3063–3072. (d) Demonceau, A.; Stumpf, A. W.; Saive, E.; Noels, A. F. *Macromolecules* **1997**, 3127–3136.

(C_{benzene}); 122.27 (d, ³J_{CP} = 7.8 Hz, C_m); 152.39 (C_o); 152.95 (C_p); 165.76 (C_i). ¹⁹F NMR (188.3 MHz): δ -71.90 (s). ¹¹B NMR (96.3 MHz): δ -0.18 (br s). Anal. Calcd for C₄₂H₆₉BF₄P₂Ru: C, 61.23; H, 8.44. Found: C, 60.99; H, 8.62.

[(η⁶-*p*-Cymene)(PCy₃)Ru(PHMes*)]BPh₃OH (**3aBPh₃OH**). To a green solution of **2a** (0.244 g, 0.31 mmol) in toluene (10 mL) was added 0.074 g of BPh₃ (0.31 mmol). In the presence of water (6 μL, 0.31 mmol), the solution turned slowly to violet, and the mixture was stirred for 24 h at room temperature. The volatiles were removed *in vacuo*, leaving a violet residue. Trituration with pentane afforded pure **3aBPh₃OH** as a violet powder (0.288 g, 87%). Mp: 198 °C. ³¹P NMR (81.015 MHz): δ 45.15 (dd; ²J_{PP} = 83.9 Hz; ³J_{HP} = 19.0 Hz; PCy₃); 186.32 (dd; ¹J_{PH} = 341.1 Hz; ²J_{PP} = 83.9 Hz; PHMes*). ¹H NMR (200.132 MHz): δ 1.00 (d; ³J_{HH} = 6.7 Hz; 6H; C₁-CH-(CH₃)₂); 1.26 (m; 12H; C_oH₂); 1.37 (s; 9H; C_p-C-(CH₃)₃); 1.48 (s; 18H; C_o-C-(CH₃)₃); 1.70 (s; 3H; C₄-CH₃); 1.83 (m; 6H; C_dH₂); 2.24 (m; 12H; C_bH₂); 2.74 (m; 4H; C_aH and C₁-CH-(CH₃)₂); 4.81 (m; 4H; C₂H and C₃H); 6.98 (m; 9H; C_bH_{Ph} and C_dH_{Ph}); 7.44 (s; 2H; C_mH); 7.71 (m; 6H; C_cH_{Ph}); 9.00 (dd; ¹J_{HP} = 341.1 Hz; ³J_{HP} = 19.0 Hz; 1H; PH). ¹³C{¹H} NMR (50.323 MHz): δ 18.19 (s; C₄-CH₃); 23.58 (s; C₁-CH-(CH₃)₂); 26.37 (s; C_d); 27.51 (d; ³J_{CP} = 11.1 Hz; C_o); 30.01 (s; C_b); 30.94 (s; C₁-CH-(CH₃)₂); 31.20 (s; C_p-C-(CH₃)₃); 32.64 (s; C_o-C-(CH₃)₃); 34.22 (d; ¹J_{CP} = 50.9 Hz; C_a); 35.28 (s; C_p-C-(CH₃)₃); 38.70 (s; C_o-C-(CH₃)₃); 83.76 (s; C₃); 87.99 (s; C₂); 99.45 (d; ²J_{CP} = 3.4 Hz; C_d); 112.66 (d; ²J_{CP} = 2.8 Hz; C₁); 122.34 (d; ³J_{CP} = 8.3 Hz; C_m); 127.25 (s; C_{bPh}); 128.29 (s; C_{aPh}); 131.96 (s; C_{dPh}); 134.90 (s; C_{cPh}); 152.40 (s; C_o); 153.06 (s; C_p); 159.05 (s; C_i). ¹¹B NMR (96.29 MHz): δ 1.43 (br s). Anal. Calcd for C₆₄H₉₃BOP₂Ru: C, 73.05; H, 8.91. Found: C, 73.26; H, 9.02.

[(η⁶-Benzene)(PCy₃)Ru(PHMes*)]BPh₃OH (**3bBPh₃OH**). A similar procedure to that described for **3aBPh₃OH** was used. **2b** (0.057 g, 0.08 mmol), BPh₃ (0.019 g, 0.08 mmol), and H₂O (2 μL, 0.08 mmol) gave **3bBPh₃OH** as a violet solid (0.063 g, 83%). Mp: 167 °C. ³¹P NMR (81.015 MHz): δ 48.07 (d; ²J_{PP} = 83.9 Hz; ³J_{HP} = 18.7 Hz; PCy₃); 199.13 (dd; ¹J_{PH} = 350.0 Hz; ²J_{PP} = 83.9 Hz; PHMes*). ¹H NMR (300.13 MHz): δ 1.27 (m; 12H; C_oH₂); 1.38 (s; 9H; C_p-C-(CH₃)₃); 1.45 (s; 18H; C_o-C-(CH₃)₃); 1.75 (m; 6H; C_dH₂); 2.21 (m; 12H; C_bH₂); 2.75 (m; 3H; C_aH); 4.85 (s; 6H; CH_{benzene}); 7.02 (m; 9H; C_bH_{Ph} et C_dH_{Ph}); 7.42 (s; 2H; C_mH); 7.94 (m; 6H; C_cH_{Ph}); 8.99 (dd; ¹J_{HP} = 350.0 Hz; ³J_{HP} = 18.7 Hz; 1H; PH). ¹³C{¹H} NMR (75.468 MHz): δ 26.40 (s; C_d); 27.51 (d; ³J_{CP} = 11.2 Hz; C_o); 30.14 (s; C_b); 31.17 (s; C_p-C-(CH₃)₃); 32.45 (s; C_o-C-(CH₃)₃); 33.86 (d; ¹J_{CP} = 48.5 Hz; C_a); 35.28 (s; C_p-C-(CH₃)₃); 38.47 (s; C_o-C-(CH₃)₃); 86.64 (s; C_{benzene}); 122.51 (d; ³J_{CP} = 8.8 Hz; C_m); 127.15 (s; C_{bPh}); 128.28 (s; C_{aPh}); 132.65 (s; C_{dPh}); 135.02 (s; C_{cPh}); 152.32 (s; C_o); 153.55 (s; C_p); 160.77 (s; C_i). ¹¹B NMR (96.29 MHz): δ 1.52 (s). Anal. Calcd for C₆₀H₇₅BOP₂Ru: C, 73.08; H, 7.67. Found: C, 73.14; H, 8.00.

(η⁶-*p*-Cymene)(PCy₃)Ru[P(BH₃)Mes*] (**4a**). To a green solution of **2a** (0.087 g, 0.11 mmol) in toluene (5 mL) was added an excess of BH₃·SMe₂ (1.1 mmol, 2 M in toluene). The solution turned slowly to violet, and the mixture was stirred for 15 min at room temperature. The volatiles were removed *in vacuo*, and pure **4a** was obtained as an oily violet residue (0.080 g, 90%). ³¹P NMR (81.0 MHz): δ 48.69 (d, ²J_{PP} = 68.7 Hz, PCy₃); 506.27 (d, ²J_{PP} = 68.7 Hz, P(BH₃)). ¹H NMR (200.1 MHz): δ 1.05 (d, ³J_{HH} = 6.9 Hz, 6H, C₁-CH-(CH₃)₂); 1.35 (m, 12H, C_oH₂); 1.46 (s, 9H, C_p-C-(CH₃)₃); 1.54 (m, 12H, C_bH₂); 1.83 (s, 18H, C_o-C-(CH₃)₃); 2.02 (s, 3H, C₄-CH₃); 2.16 (m, 6H, C_dH₂); 2.70 (m, 4H, C_aH and C₁-CH-(CH₃)₂); 4.55 (m, 4H, C₂H and C₃H); 7.65 (s, 2H, C_mH). ¹³C{¹H} NMR (75.5 MHz): δ 19.23 (C₄-CH₃); 25.68 (C₁-CH-(CH₃)₂); 28.28 (C_d); 30.49 (br s; C_c); 30.77 (C_b); 31.09 (C₁-CH-(CH₃)₂); 31.45 (C_p-C-(CH₃)₃); 33.51 (C_o-C-(CH₃)₃); 34.90 (C_p-C-(CH₃)₃); 35.31 (br s; C_a); 40.11 (C_o-C-(CH₃)₃); 81.01 (C₃); 85.63 (C₂); 89.12 (C₄); 103.05 (C₁); 119.25 (C_m); 144.85 (C_p); 145.51 (C_o). ¹¹B NMR (96.3 MHz): δ 18.33 (br s).

(η⁶-Benzene)(PCy₃)Ru[P(BH₃)Mes*] (**4b**). A similar procedure to that described for **4a** was used. **2b** (0.089 g, 0.11 mmol) and BH₃·SMe₂ (1.1 mmol, 2 M in toluene) gave **4b** as an oily violet residue (0.069 g, 83%). ³¹P NMR (81.0 MHz): δ 48.40 (d, ²J_{PP} = 68.7 Hz, PCy₃); 521.06 (d, ²J_{PP} = 68.7 Hz, P(BH₃)). ¹H NMR (200.1 MHz): δ 1.33 (m, 12H, C_oH₂); 1.47 (s, 9H, C_p-C-(CH₃)₃); 1.59 (m, 12H, C_bH₂); 1.71 (s, 18H, C_o-C-(CH₃)₃); 1.99 (m, 6H, C_dH₂); 2.56 (m, 3H, C_aH); 4.64 (s, 6H, CH_{benzene}); 7.54 (s, 2H, C_mH). ¹³C{¹H} NMR (75.5 MHz): δ 27.20 (C_d); 29.12 (br s, C_c); 29.80 (C_b); 30.22 (C_p-C-(CH₃)₃); 31.41 (C_o-C-(CH₃)₃); 33.90 (br s, C_a); 37.01 (C_p-C-(CH₃)₃); 41.04 (C_o-C-(CH₃)₃); 80.43 (C_{benzene}); 118.26 (C_m); 144.53 (C_p); 146.05 (C_o). ¹¹B NMR (96.3 MHz): δ 18.29 (br s).

[(η⁶-*p*-Cymene)(PCy₃)Ru(PMeMes*)]I (**5a**). To a green solution of **2a** (0.658 g, 0.83 mmol) in toluene (10 mL) was added MeI (0.052 mL, 0.83 mmol). The solution turned slowly to violet, and the mixture was stirred for 1 h at room temperature. The volatiles were removed *in vacuo*. Trituration with pentane afforded pure **5a** as a violet powder (0.737 g, 95%). Mp: 160 °C. ³¹P NMR (81.0 MHz): δ 48.80 (d, ²J_{PP} = 82.1 Hz, PCy₃); 240.38 (dq, ²J_{PP} = 82.1 Hz, ²J_{PH} = 9.7 Hz, PMeMes*). ¹H NMR (200.1 MHz): δ 1.08 (d, ³J_{HH} = 6.9 Hz, 3H, C₁-CH-CH₃); 1.32 (d, ³J_{HH} = 6.9 Hz, 3H, C₁-CH-CH₃); 1.43 (s, 9H, C_p-C-(CH₃)₃); 1.46 (s, 9H, C_o-C-(CH₃)₃); 1.52 (s, 9H, C_o-C-(CH₃)₃); 1.56 (s, 3H, C₄-CH₃); 1.86 (m, 12H, C_oH₂); 2.13 (d, ²J_{HP} = 9.7 Hz, 3H, P-CH₃); 2.26 (m, 6H, C_dH₂); 2.56 (m, 12H, C_bH₂); 3.27 (m, 4H, C_aH and C₁-CH-(CH₃)₂); 3.73 (s, 1H, C₂H); 4.77 (s, 1H, C₃H); 5.43 (s, 2H, C₂H and C₃H); 7.54 (s, 1H, C_mH); 7.65 (s, 1H, C_mH). ¹³C{¹H} NMR (50.3 MHz): δ 18.60 (C₄-CH₃); 21.48 (C₁-CH-(CH₃)₂); 26.31 (C_d); 27.65 (d, ³J_{CP} = 9.2 Hz, C_o); 30.25 (C_b); 30.58 (C₁-CH-(CH₃)₂); 31.09 (C_o-C-(CH₃)₃); 31.26 (C_p-C-(CH₃)₃); 32.41 (d, ¹J_{CP} = 7.4 Hz, C_a); 34.64 (br s, P-CH₃); 35.10 (C_p-C-(CH₃)₃); 39.67 (C_o-C-(CH₃)₃); 79.54 (C₃); 83.99 (C₂); 100.97 (d, ²J_{CP} = 6.5 Hz, C_d); 112.96 (d, ²J_{CP} = 5.6 Hz, C₁); 123.56 (d, ³J_{CP} = 7.4 Hz, C_m); 144.94 (d, ²J_{CP} = 13.9 Hz, C_o); 149.36 (C_p); 152.16 (d, ²J_{CP} = 2.0 Hz, C_o); 166.82 (C_i). Anal. Calcd for C₄₇H₇₉IP₂Ru: C, 60.44; H, 8.53. Found: C, 59.95; H, 8.17.

[(η⁶-Benzene)(PCy₃)Ru(PMeMes*)]I (**5b**). A similar procedure to that described for **5a** was used. **2b** (0.610 g; 0.83 mmol) and MeI (0.052 mL, 0.83 mmol) gave **5b** as a violet solid (0.641 g, 88%). Mp: 144 °C. ³¹P NMR (81.0 MHz): δ 51.89 (d, ²J_{PP} = 76.3 Hz, PCy₃); 248.19 (dd, ²J_{PH} = 10.2 Hz, ²J_{PP} = 76.3 Hz, PMeMes*). ¹H NMR (200.1 MHz): δ 1.36 (s, 9H, C_p-C-(CH₃)₃); 1.56 (s, 18H, C_o-C-(CH₃)₃); 1.85 (m, 12H, C_oH₂); 2.21 (d, ²J_{HP} = 10.2 Hz, 3H, P-CH₃); 2.33 (m, 6H, C_dH₂); 3.14 (m, 12H, C_bH₂); 3.67 (m, 3H, C_aH); 5.31 (s, 6H, CH_{benzene}); 7.51 (s, 2H, C_mH). ¹³C{¹H} NMR (50.3 MHz): δ 26.44 (C_d); 27.77 (d, ³J_{CP} = 10.2 Hz, C_o); 30.36 (C_b); 31.11 (C_p-C-(CH₃)₃); 31.52 (C_o-C-(CH₃)₃); 34.29 (br s, P-CH₃); 34.75 (d, ¹J_{CP} = 3.7 Hz, C_a); 35.17 (s, C_p-C-(CH₃)₃); 39.31 (s, C_o-C-(CH₃)₃); 87.42 (d, ²J_{CP} = 3.7 Hz, C_{benzene}); 123.52 (d, ³J_{CP} = 8.3 Hz, C_m); 146.12 (d, ²J_{CP} = 15.7 Hz, C_o); 149.95 (C_p); 152.47 (d, ²J_{CP} = 2.0 Hz, C_o); 166.56 (d, ¹J_{CP} = 44.4 Hz, C_i). Anal. Calcd for C₄₃H₇₁IP₂Ru: C, 58.83; H, 8.15. Found: C, 58.42; H, 8.07.

(η⁶-*p*-Cymene)Ru[η³-P(CH=CHSiMe₃)Mes*] (**6**). To a green solution of **2a** (0.214 g, 0.27 mmol) in toluene (10 mL) was added Me₃SiC≡CH (0.040 mL, 0.29 mmol). The solution turned to orange, and the mixture was stirred for 1 h at room temperature. The volatiles were removed *in vacuo*. The residue was extracted with pentane, filtered, and concentrated. Upon standing at -20 °C, **6** was obtained as a pure orange solid (0.156 g, 95%). Mp: 82 °C. ³¹P NMR (81.0 MHz): δ -2.76 (m). ¹H NMR (400.1 MHz): δ 0.23 (s, 9H, Si(CH₃)₃); 1.17 (s, 3H, P-CH₂-C-CH₃); 1.25 (s, 3H, P-CH₂-C-CH₃); 1.27 (br s, 2H, P-CH₂); 1.32 (s, 9H, C_p-C-(CH₃)₃); 1.36 (d, ³J_{HH} = 6.8 Hz, 3H, C₁-CH-CH₃); 1.38 (d, ³J_{HH} = 6.6 Hz, 3H, C₁-CH-CH₃); 1.79 (s, 9H, C_o-C-(CH₃)₃); 2.10 (s, 3H, C₄-CH₃); 2.42 (d, ³J_{HH} = 7.4 Hz, 1H, P-CH=CH); 2.66

(dd, $^2J_{HP} = 21.8$ Hz, $^3J_{HH} = 7.4$ Hz, 1H, P-CH=CH); 3.44 (m, 1H, C₁-CH-(CH₃)₂); 4.28 (d, $^3J_{HP} = 5.5$ Hz, 1H, C₂H); 5.01 (d, $^3J_{HP} = 5.1$ Hz, 1H, C₃H); 5.09 (d, $^3J_{HP} = 5.7$ Hz, 1H, C₂H); 5.79 (d, $^3J_{HP} = 5.5$ Hz, 1H, C₃H); 7.22 (d, $^4J_{HH} = 1.8$ Hz, 1H, C_mH); 7.56 (dd, $^4J_{HP} = 4.9$ Hz, $^4J_{HH} = 1.8$ Hz, 1H, C_mH). $^{13}\text{C}\{^1\text{H}\}$ NMR (100.6 MHz): δ 0.34 (Si(CH₃)₃); 19.34 (C₄-CH₃); 25.83 (C₁-CH-CH₃); 26.36 (C₁-CH-CH₃); 28.66 (P-CH₂-C-CH₃); 30.55 (d, $^3J_{CP} = 9.3$ Hz, P-CH₂-C-CH₃); 31.34 (C₁-CH-(CH₃)₂); 31.51 (C_p-C-(CH₃)₃); 32.52 (C_o-C-(CH₃)₃); 33.18 (P-CH=CH); 34.50 (d, $^1J_{CP} = 17.6$ Hz, P-CH₂); 35.15 (C_p-C-(CH₃)₃); 37.78 (d, $^1J_{CP} = 10.2$ Hz, P-CH=CH); 37.94 (C_o-C-(CH₃)₃); 41.42 (d, $^2J_{CP} = 6.5$ Hz, C_o-C-(CH₃)₂); 72.71 (d, $^2J_{CP} = 9.3$ Hz, C₂); 74.64 (C₃); 81.35 (C₃); 82.85 (C₂); 99.02 (d, $^2J_{CP} = 4.6$ Hz, C₄); 110.25 (C₁); 118.25 (d, $^3J_{CP} = 7.4$ Hz, C_m); 121.95 (d, $^3J_{CP} = 8.3$ Hz, C_m); 126.05 (d, $^1J_{CP} = 32.4$ Hz, C_i); 153.13 (d, $^4J_{CP} = 1.9$ Hz, C_p); 153.77 (d, $^2J_{CP} = 9.3$ Hz, C_o-C-(CH₃)₃); 159.73 (d, $^2J_{CP} = 12.0$ Hz, C_o-C-(CH₃)₂). Anal. Calcd for C₃₃H₅₃PRuSi: C, 64.99; H, 8.76. Found: C, 64.78; H, 8.69.

Upon exposure to air, complex **6** is oxidized and converted into the corresponding phosphine oxide. ^{31}P NMR (81.0 MHz): δ 33.24 (t, $^2J_{HP} = 14.4$ Hz). ^1H NMR (400.1 MHz): δ 0.14 (s, 9H, Si(CH₃)₃); 1.34 (s, 9H, C_p-C-(CH₃)₃); 1.52 (s, 6H, P-CH₂-C-CH₃); 1.58 (s, 9H, C_o-C-(CH₃)₃); 2.19 (d, $^2J_{HP} = 14.4$ Hz, 2H, P-CH₂); 6.84 (dd, $^3J_{HH} = 19.8$ Hz, $^2J_{HP} = 31.3$ Hz, 1H, P-CH=CH); 7.28–7.54 (m, 3H, C_mH and P-CH=CH).

(η^6 -*p*-Cymene)Ru(η^3 -P(CH=CHPh)Mes*) (**7**). A similar procedure to that described for **6** was used. **2a** (0.412 g; 0.52 mmol) and PhC \equiv CH (0.059 mL, 0.54 mmol) gave **7** as a red-orange solid (0.306 g, 96%). Mp: 192 °C. ^{31}P NMR (81.0 MHz): δ -10.40 (m). ^1H NMR (400.1 MHz): δ 1.28 (s, 3H, P-CH₂-C-CH₃); 1.37 (s, 3H, P-CH₂-C-CH₃); 1.42 (s, 9H, C_p-C-(CH₃)₃); 1.43 (d, $^3J_{HH} = 6.6$ Hz, 3H, C₁-CH-CH₃); 1.44 (d, $^3J_{HH} = 6.9$ Hz, 3H, C₁-CH-CH₃); 1.46 (br s, 2H, P-CH₂); 1.97 (s, 9H, C_o-C-(CH₃)₃); 2.14 (s, 3H, C₄-CH₃); 2.79 (m, 1H, C₁-CH-(CH₃)₂); 3.03 (dd, $^2J_{HP} = 15.4$ Hz, $^3J_{HH} = 5.4$ Hz, 1H, P-CH=CH); 3.23 (d, $^3J_{HP} = 5.5$ Hz, 1H, C₃H); 3.26 (d, $^3J_{HH} = 5.4$ Hz, 1H, P-CH=CH); 4.90 (d, $^3J_{HP} = 4.4$ Hz, 1H, C₂H); 5.21 (d, $^3J_{HP} = 5.5$ Hz, 1H, C₃H); 5.42 (d, $^3J_{HP} = 5.5$ Hz, 1H, C₂H); 7.24 (m, 2H, C_hH); 7.46 (d, $^4J_{HH} = 2.0$ Hz, 1H, C_mH); 7.48 (s, 3H, C_hH and C_dH); 7.86 (dd, $^4J_{HP} = 4.9$ Hz, $^4J_{HH} = 2.0$ Hz, 1H, C_mH). $^{13}\text{C}\{^1\text{H}\}$ NMR (100.6 MHz): δ 19.82 (C₄-CH₃); 25.55 (C₁-CH-CH₃); 26.09 (C₁-CH-CH₃); 29.20 (P-CH₂-C-CH₃); 30.37 (d, $^3J_{CP} = 9.1$ Hz, P-CH₂-C-CH₃); 31.44 (C_p-C-(CH₃)₃); 32.51 (C₁-CH-(CH₃)₂); 33.29 (C_o-C-(CH₃)₃); 33.51 (P-CH=CH); 35.12 (C_p-C-(CH₃)₃); 35.67 (d, $^1J_{CP} = 17.5$ Hz, P-CH₂); 37.13 (d, $^1J_{CP} = 8.2$ Hz, P-CH=CH); 37.99 (C_o-C-(CH₃)₃); 41.73 (d, $^2J_{CP} = 6.5$ Hz, C_o-C-(CH₃)₂); 76.68 (C₂); 80.80 (d, $^2J_{CP} = 5.3$ Hz, C₃); 81.50 (d, $^2J_{CP} = 5.3$ Hz, C₃); 82.69 (C₂); 98.06 (d, $^2J_{CP} = 4.2$ Hz, C₄); 110.02 (C₁); 118.25 (d, $^3J_{CP} = 8.3$ Hz, C_m); 122.11 (d, $^3J_{CP} = 8.4$ Hz, C_m); 122.98 (C_i); 125.97 (C_b); 128.31 (C_d); 152.09 (d, $^2J_{CP} = 16.2$ Hz, C_a); 153.36 (C_p); 154.24 (d, $^2J_{CP} = 9.6$ Hz, C_o-C-(CH₃)₃); 160.46 (d, $^2J_{CP} = 12.5$ Hz, C_o-C-(CH₃)₂). Anal. Calcd for C₃₆H₄₉PRu: C, 70.44; H, 8.05. Found: C, 70.51; H, 8.09.

Upon exposure to air, complex **7** is oxidized and converted into the corresponding phosphine oxide. ^{31}P NMR (81.0 MHz): δ 32.46 (t, $^2J_{HP} = 14.0$ Hz). ^1H NMR (400.1 MHz): δ 1.33 (s, 9H, C_p-C-(CH₃)₃); 1.51 (s, 6H, P-CH₂-C-CH₃); 1.58 (s, 9H, C_o-C-(CH₃)₃); 2.23 (d, $^2J_{HP} = 14.0$ Hz, 2H, P-CH₂); 6.84 (dd, $^3J_{HH} = 20.2$ Hz, $^2J_{HP} = 30.8$ Hz, 1H, P-CH=CH); 7.16–7.72 (m, 8H, C_mH and Ph and P-CH=CH).

(η^6 -*p*-Cymene)(PPh₃)Ru(PMes*) (**8**). A similar procedure to that described for **2a** was used. (η^6 -*p*-Cymene)(PPh₃)RuCl₂ (0.102 g; 0.16 mmol), Mes*PH₂ (0.042 g; 0.150 mmol), and DBU (0.041 mL; 0.29 mmol) gave **8** as a green solid (0.117 g, 94%). Mp: 120 °C dec. ^{31}P NMR (81.0 MHz): δ 38.75 (d, $^2J_{PP} = 45.8$ Hz, PPh₃); 835.36 (d, $^2J_{PP} = 45.8$ Hz, PMes*). ^1H NMR (400.1 MHz): δ 0.93 (d, $^3J_{HH} = 6.6$ Hz, 6H, C₁-CH-(CH₃)₂); 1.54 (s, 9H, C_p-C-

(CH₃)₃); 1.63 (s, 18H, C_o-C-(CH₃)₃); 1.77 (s, 3H, C₄-CH₃); 2.42 (m, 1H, C₁-CH-(CH₃)₂); 4.58 (AB, $^3J_{HH} = 6.1$ Hz, 2H, C₃H); 4.61 (AB, $^3J_{HH} = 6.1$ Hz, 2H, C₂H); 7.12 (br s, 9H, C_hH and C_dH); 7.54 (br s, 2H, C_mH); 7.94 (m, 6H, C_hH). $^{13}\text{C}\{^1\text{H}\}$ NMR (100.6 MHz): δ 18.94 (C₄-CH₃); 24.36 (C₁-CH-(CH₃)₂); 30.79 (C₁-CH-(CH₃)₂); 31.95 (C_p-C-(CH₃)₃); 32.84 (d, $^4J_{CP} = 6.4$ Hz, C_o-C-(CH₃)₃); 34.91 (C_p-C-(CH₃)₃); 38.66 (C_o-C-(CH₃)₃); 84.65 (d, $^2J_{CP} = 2.8$ Hz, C₂); 87.22 (d, $^2J_{CP} = 2.8$ Hz, C₃); 91.47 (C₄); 105.02 (C₁); 119.39 (C_m); 127.73 (C_b); 129.14 (C_d); 135.30 (d, $^3J_{CP} = 11.1$ Hz, C_i); 139.64 (d, $^1J_{CP} = 38.8$ Hz, C_a); 145.67 (C_p); 145.85 (C_o); 183.59 (C_i). Anal. Calcd for C₄₆H₅₈P₂Ru: C, 71.38; H, 7.55. Found: C, 71.48; H, 7.73.

(η^6 -*p*-Cymene)[P(*p*-ClC₆H₄)₃]Ru(PMes*) (**9**). An NMR tube was charged with **2a** (0.022 g, 0.28 mmol) and P(*p*-ClC₆H₄)₃ (0.010 g, 0.28 mmol) in C₆D₆ (0.5 mL). The tube was maintained at 45 °C and monitored by ^1H NMR. Data for (η^6 -*p*-cymene)[P(*p*-ClC₆H₄)₃]Ru(PMes*) (**9**). ^{31}P NMR (81.0 MHz): δ 37.15 (d, $^2J_{PP} = 45.8$ Hz, P(*p*-ClC₆H₄)₃); 843.17 (d, $^2J_{PP} = 45.8$ Hz, PMes*). ^1H NMR (200.1 MHz): δ 0.86 (d, $^3J_{HH} = 6.8$ Hz, 6H, C₁-CH-(CH₃)₂); 1.51 (s, 9H, C_p-C-(CH₃)₃); 1.57 (s, 18H, C_o-C-(CH₃)₃); 1.88 (s, 3H, C₄-CH₃); 2.32 (m, 1H, C₁-CH-(CH₃)₂); 4.48 (AB, $^3J_{HH} = 6.4$ Hz, 2H, C₃H); 4.52 (AB, $^3J_{HH} = 6.4$ Hz, 2H, C₂H); 7.19 (d, $^3J_{HP} = 7.4$ Hz, 6H, C_bH); 7.55 (s, 2H, C_mH); 7.62 (br s, 6H, C_hH).

(η^6 -*p*-Cymene)[P(*p*-MeC₆H₄)₃]Ru(PMes*) (**10**). An NMR tube was charged with **2a** (0.025 g, 0.32 mmol) and P(*p*-tolyl)₃ (0.010 g, 0.32 mmol) in C₆D₆ (0.5 mL). The tube was maintained at 45 °C and monitored by ^1H NMR. Data for (η^6 -*p*-cymene)[P(*p*-MeC₆H₄)₃]Ru(PMes*) (**10**). ^{31}P NMR (81.0 MHz): δ 36.40 (d, $^2J_{PP} = 45.8$ Hz, P(*p*-tolyl)₃); 831.97 (d, $^2J_{PP} = 45.8$ Hz, PMes*). ^1H NMR (200.1 MHz): δ 0.98 (d, $^3J_{HH} = 6.8$ Hz, 6H, C₁-CH-(CH₃)₂); 1.56 (s, 9H, C_p-C-(CH₃)₃); 1.67 (s, 18H, C_o-C-(CH₃)₃); 1.83 (s, 3H, C₄-CH₃); 2.10 (s, 9H, C_d-CH₃); 2.57 (m, 1H, C₁-CH-(CH₃)₂); 4.62 (AB, $^3J_{HH} = 6.6$ Hz, 2H, C₃H); 4.66 (AB, $^3J_{HH} = 6.6$ Hz, 2H, C₂H); 7.06 (d, $^3J_{HP} = 7.2$ Hz, 6H, C_bH); 7.55 (s, 2H, C_mH); 7.92 (br s, 6H, C_hH).

(η^6 -*p*-Cymene)[P(*p*-MeOC₆H₄)₃]Ru(PMes*) (**11**). An NMR tube was charged with **2a** (0.025 g, 0.32 mmol) and P(*p*-MeOC₆H₄)₃ (0.011 g, 0.32 mmol) in C₆D₆ (0.5 mL). The tube was maintained at 45 °C and monitored by ^1H NMR. Data for (η^6 -*p*-cymene)[P(*p*-MeOC₆H₄)₃]Ru(PMes*) (**11**). ^{31}P NMR (81.0 MHz): δ 34.51 (d, $^2J_{PP} = 45.8$ Hz, P(*p*-MeOC₆H₄)₃); 830.36 (d, $^2J_{PP} = 45.8$ Hz, PMes*). ^1H NMR (200.1 MHz): δ 0.98 (d, $^3J_{HH} = 6.8$ Hz, 6H, C₁-CH-(CH₃)₂); 1.55 (s, 9H, C_p-C-(CH₃)₃); 1.67 (s, 18H, C_o-C-(CH₃)₃); 1.84 (s, 3H, C₄-CH₃); 2.54 (m, 1H, C₁-CH-(CH₃)₂); 3.30 (s, 9H, C_d-OCH₃); 4.61 (AB, $^3J_{HH} = 6.2$ Hz, 2H, C₃H); 4.69 (AB, $^3J_{HH} = 6.2$ Hz, 2H, C₂H); 6.86 (d, $^3J_{HP} = 7.8$ Hz, 6H, C_bH); 7.54 (s, 2H, C_mH); 7.92 (br s, 6H, C_hH).

(η^6 -*p*-Cymene)[P(NC₄H₄)₃]Ru(PMes*) (**12**). A similar procedure to that described for **2a** was used. (η^6 -*p*-Cymene)[P(NC₄H₄)₃]RuCl₂ (0.436 g; 0.72 mmol), Mes*PH₂ (0.194 g; 0.70 mmol), and DBU (0.210 mL; 1.4 mmol) gave **12** as a green solid (0.412 g, 80%). Mp: 131 °C. ^{31}P NMR (81.0 MHz): δ 95.16 (d, $^2J_{PP} = 15.3$ Hz, P(NC₄H₄)₃); 886.77 (d, $^2J_{PP} = 15.3$ Hz, PMes*). ^1H NMR (200.1 MHz): δ 0.83 (d, $^3J_{HH} = 6.8$ Hz, 3H, C₁-CH-CH₃); 1.16 (d, $^3J_{HH} = 6.8$ Hz, 3H, C₁-CH-CH₃); 1.30 (s, 3H, C₄-CH₃); 1.48 (s, 9H, C_p-C-(CH₃)₃); 1.56 (s, 18H, C_o-C-(CH₃)₃); 2.64 (m, $^3J_{HH} = 6.8$ Hz, 1H, C₁-CH-(CH₃)₂); 4.67 (AB, $^3J_{HH} = 6.6$ Hz, 2H, C₃H); 4.79 (AB, $^3J_{HH} = 6.6$ Hz, 2H, C₂H); 6.33 (br s, 6H, C_hH); 7.18 (br s, 6H, C_bH); 7.54 (d, $^4J_{HH} = 2.0$ Hz, 2H, C_mH). $^{13}\text{C}\{^1\text{H}\}$ NMR (50.3 MHz): δ 19.16 (C₄-CH₃); 24.12 (C₁-CH-CH₃); 24.36 (C₁-CH-CH₃); 30.81 (C₁-CH-(CH₃)₂); 31.53 (C_p-C-(CH₃)₃); 31.82 (C_o-C-(CH₃)₃); 34.87 (C_p-C-(CH₃)₃); 38.57 (C_o-C-(CH₃)₃); 89.29 (d, $^2J_{CP} = 4.6$ Hz, C₃); 91.56 (d, $^2J_{CP} = 3.7$ Hz, C₂); 97.85 (C₄); 110.69 (C₁); 111.82 (d, $^3J_{CP} = 5.6$ Hz, C_i); 119.64 (C_m); 125.50 (d, $^2J_{CP} = 8.3$ Hz, C_b); 146.14 (C_p); 146.73

(C_o); 154.43 (d, ¹J_{CP} = 7.4 Hz, C_i). Anal. Calcd for C₄₀H₅₅N₃P₂-Ru: C, 64.84; H, 7.48. Found: C, 65.01; H, 7.52.

(*η*⁶-*p*-Cymene)[P(*m*-MeC₆H₄)₃]Ru(PMes*) (**13**). A similar procedure to that described for **2a** was used. (*η*⁶-*p*-Cymene)[P(*m*-MeC₆H₄)₃]RuCl₂ (0.253 g; 0.37 mmol), Mes*PH₂ (0.092 g; 0.33 mmol), and DBU (0.099 mL; 0.66 mmol) gave **13** as a green solid (0.246 g, 92%). Mp: 137 °C. ³¹P NMR (81.0 MHz): δ 38.78 (d, ²J_{PP} = 45.8 Hz, P(*m*-tolyl)₃); 832.77 (d, ²J_{PP} = 45.8 Hz, PMes*). ¹H NMR (400.1 MHz): δ 0.99 (d, ³J_{HH} = 6.8 Hz, 6H, C₁-CH-(CH₃)₂); 1.55 (s, 9H, C_p-C-(CH₃)₃); 1.63 (s, 18H, C_o-C-(CH₃)₃); 1.82 (s, 3H, C₄-CH₃); 2.15 (s, 9H, C_c-CH₃); 2.59 (m, 1H, C₁-CH-(CH₃)₂); 4.59 (AB, ³J_{HH} = 6.4 Hz, 2H; C₃H); 4.71 (AB, ³J_{HH} = 6.4 Hz, 2H, C₂H); 6.97 (d, ³J_{HH} = 7.8 Hz, 3H, C_dH); 7.10 (t, ³J_{HH} = 7.7 Hz, 3H, C_eH); 7.52 (s, 2H, C_mH); 7.71 (t, ³J_{HP} = 8.4 Hz, 3H, C_fH); 7.97 (d, ³J_{HP} = 10.6 Hz, 3H, C_bH). ¹³C{¹H} NMR (100.6 MHz): δ 18.98 (C₄-CH₃); 21.68 (C_c-CH₃); 24.40 (C₁-CH-CH₃); 30.88 (C₁-CH-(CH₃)₂); 31.97 (C_p-C-(CH₃)₃); 32.78 (C_o-C-(CH₃)₃); 34.91 (C_p-C-(CH₃)₃); 38.71 (C_o-C-(CH₃)₃); 84.62 (d, ²J_{CP} = 2.0 Hz, C₃); 87.30 (d, ²J_{CP} = 2.0 Hz, C₂); 91.03 (C₄); 104.67 (C₁); 119.22 (C_m); 127.60 (d, ³J_{CP} = 9.4 Hz, C_e); 129.92 (C_d); 132.10 (d, ²J_{CP} = 9.2 Hz, C_f); 136.34 (d, ²J_{CP} = 13.9 Hz, C_b); 137.04 (d, ³J_{CP} = 10.2 Hz, C_c); 139.67 (d, ¹J_{CP} = 37.9 Hz, C_a); 145.50 (C_p); 145.85 (C_o); 154.44 (d, ¹J_{CP} = 6.5 Hz, C_i). Anal. Calcd for C₄₉H₆₄P₂Ru: C, 72.12; H, 7.91. Found: C, 71.98; H, 7.83.

Kinetic Measurements for Phosphine Substitution Reactions. NMR tubes (5 mm) were charged with appropriate amounts of complexes and phosphines, and C₆D₆ was added to a total volume of 0.5 mL. The tube was maintained at 45 °C and monitored by ¹H NMR.

X-ray Diffraction Structure Analysis. Data for all structures presented in this paper were collected at low temperatures using an oil-coated shock-cooled crystal on a Bruker-AXS CCD 1000 diffractometer with Mo K α radiation (λ = 0.71073 Å). The structures were solved by direct methods,⁵² and all non hydrogen atoms were refined anisotropically using the least-squares method

on F^2 .⁵³ Very small crystals of poor quality are responsible for insufficient reflections and the low quality of the structure analysis.

2a: C₄₆H₇₆P₂Ru, M = 792.08, monoclinic, $P2_1/c$, a = 10.359(5) Å, b = 22.300(10) Å, c = 19.612(8) Å, β = 102.577(11)°, V = 4422(3) Å³, Z = 4, T = 193(2) K; 17 133 reflections (5318 independent, R_{int} = 0.3085) were collected. Largest electron density residue: 0.598 e Å⁻³, R_1 (for $I > 2\sigma(I)$) = 0.0909 and wR_2 = 0.2229 (all data) with $R_1 = \sum||F_o| - |F_c||/\sum|F_o|$ and $wR_2 = (\sum w(F_o^2 - F_c^2)^2/\sum w(F_o^2))^0.5$.

2b: C₄₂H₆₈P₂Ru, M = 735.97, triclinic, $P\bar{1}$, a = 10.385(13) Å, b = 15.164(18) Å, c = 15.641(19) Å, α = 61.91(2)°, β = 73.53(2)°, γ = 78.16(2)°, V = 2076(4) Å³, Z = 2, T = 133(2) K; 5831 reflections (3286 independent, R_{int} = 0.3049) were collected. Largest electron density residue: 1.372 e Å⁻³, R_1 (for $I > 2\sigma(I)$) = 0.1005 and wR_2 = 0.2578 (all data).

3aBF₄·C₇H₈: C₅₃H₈₁BF₄P₂Ru, M = 968.00, triclinic, $P\bar{1}$, a = 10.669(11) Å, b = 13.778(13) Å, c = 18.348(18) Å, α = 90.85(2)°, β = 95.22(2)°, γ = 99.50(2)°, V = 2648(4) Å³, Z = 2, T = 173(2) K; 9216 reflections (5434 independent, R_{int} = 0.4753) were collected. Largest electron density residue: 0.620 e Å⁻³, R_1 (for $I > 2\sigma(I)$) = 0.1102 and wR_2 = 0.2964 (all data).

Acknowledgment. This work was supported by the “Ministère de la Jeunesse, de l’Education Nationale et de la Recherche” and by the CNRS. R.M.B. is grateful to the Gabonese government for a fellowship.

Supporting Information Available: Kinetic modeling, Complete crystallographic data for compounds **2a**, **2b**, and **3aBF₄** (CIF files). This material is available free of charge via the Internet at <http://pubs.acs.org>.

OM7004854

(52) Sheldrick, G. M. *Acta Crystallogr.* **1990**, *A46*, 467–473.

(53) Sheldrick, G. M. *SHELXL-97*, Program for Crystal Structure Refinement; University of Göttingen, 1997.